Multi-asset spread option pricing and hedging

MINQIANG LI*†, JIEYUN ZHOU‡ and SHI-JIE DENG‡

†College of Management, Georgia Institute of Technology,
800 West Peachtree Street, Atlanta, GA 30308, USA
‡School of Industrial and Systems Engineering, Georgia Institute of Technology,
755 Ferst Drive NW, Atlanta, GA 30332, USA

We provide two new closed-form approximation methods for pricing spread options on a basket of risky assets: the extended Kirk approximation and the second-order boundary approximation. The latter method generalizes the results in Li *et al.* [*J. Deriv.*, 2008, **15**, 58–80] to spread options on an arbitrary number of assets. Numerical analysis shows that while the latter method is more accurate than the former, both methods are extremely fast and accurate. Closed-form approximations for important Greeks are also derived. Our approximation methods enable the accurate pricing of a bulk volume of spread options on a large number of assets in real time, which offers traders a potential edge in a dynamic market environment.

1. Introduction

Spread options are widely traded both on organized exchanges and over the counter in equity, fixed income, foreign exchange and commodity markets. They play an increasingly important role in hedging correlation risks among a set of assets of concern. In terms of the contract structure, the level of complexity rises constantly and the scope covers more and more asset classes. For instance, in the fixed income markets, instruments are traded on exchanging securities with different maturities (such as Treasury notes and bonds), with different quality levels (such as the Treasury bills and Eurodollars), and with different issuers (such as French and German bonds, or Municipal bonds and Treasury bonds). In the agricultural markets, the crush spread options traded on the Chicago Board of Trade (CBOT) exchange raw soybeans with a combination of soybean oil and soybean meal (Johnson *et al.* 1991). Asset pricing and risk management in energy markets embody a large variety of spread options (Girma and Paulson 1999). In the crude oil markets, crack spread options, which either exchange crude oil and unleaded gasoline or exchange crude oil and heating oil, are traded on the New York Mercantile Exchange (NYMEX). In the electricity markets, the spark spread option and its variants designed for exchanging one or several types of fuels for electricity are commonly utilized in hedging both short-term and long-term cross-commodity risks. Many studies have focused on spread options in different markets.

Moreover, there is a growing demand for pricing spread options involving three, four and even more assets in bulk quantity with contract parameters spanning a large range. Such scenarios arise from the application of valuing physical assets such as fossil fuel electric power plants, transmission assets (see Deng *et al.* 2001, Routledge *et al.* 2001) and natural gas storage facilities. In valuing a fossil-fuel power plant, one could approximate the plant value by a portfolio of spread options with maturity spanning 15 to 20 years. At each time instant over the life span of the plant, the owner of the plant receives a payoff resembling that of a spread option paying off the positive part of electricity price less fuel price, emission permit prices, operating and maintenance costs. If we consider the granularity in maturity to be as fine as one day, then the total number of spread option prices that need to be computed is between 5000 and 7500. Similarly, in valuing a natural gas storage facility, portfolios consisting of hundreds to thousands of daily spread options on forward contracts of different terms with maturities spanning from one year to ten years, are

---

*Corresponding author. Email: minqiang.li@mgt.gatech.edu

commonly used for approximating the facility value. In these kinds of applications, numerical algorithms that are capable of pricing large quantities of spread options on multiple assets with varying parameters fast and accurately, are in great demand. As for applications of spread options on multi-assets in the corporate finance arena, there have been proposals to use the spread between own firm's stock performance and an index level reflecting the average performance of a basket of peer firms as compensation for executives working in their own firm (see Johnson and Tian 2000).

While the spread options written on more than two underlyings are becoming more and more popular, it is very challenging to price such spread options efficiently and accurately since closed-form expressions are not available. A number of research works have studied the pricing of two-asset spread options, such as Jarrow and Rudd (1982), Wilcox (1990), Shimko (1994), Pearson (1995), Mbanefo (1997), Zhang (1997), and Carmona and Durrleman (2003). More recently, Li *et al.* (2008) provide a very accurate closed-form approximation formula for the efficient pricing of two-asset spread options. However, when the number of assets involved in the spread option is larger than two, not many approaches are available for computing the spread option price efficiently and accurately, even under the classical Black–Scholes framework. This is because when the dimension (the number of assets) is high, numerical approaches, such as numerical integration method, numerical solutions to partial differential equations and Monte Carlo simulation, often become extremely slow and inapplicable. A noticeable work that approximates the multi-asset spread option price is Carmona and Durrleman (2005). While Carmona and Durrleman's method is quite accurate, it suffers from a somewhat major shortcoming. Carmona and Durrleman's method does not give the option price in closed form. To compute each option price, one would have to solve a high-dimensional system of nonlinear equations numerically, usually by using the Newton–Raphson algorithm. However, our extensive experiments with these equations indicate that it takes considerable effort to solve them because the convergence of numerical algorithms depends very sensitively on the initial values, and a good understanding of how to choose the initial values is still lacking.

In this paper, we directly approximate multi-asset spread option prices under the jointly normal return framework based on the approximation of the exercise boundary. There are several main contributions of this paper. The most important contribution of this paper is that we give two closed-form approximation methods. The first method is an extension of Kirk's (1995) approximation for two-asset spread options to the multi-asset case. As pointed out in Li *et al.* (2008), Kirk's method can be thought of as a linear approximation of the exercise boundary. Our numerical experiment shows that in most cases, the extended Kirk approximation is quite accurate. The main advantage of the extended Kirk approximation is that it is extremely fast and robust. The second method is an extension of the

method in Li *et al.* (2008) which approximates the exercise boundary using a quadratic function. Using matrix algebra, we show that the computational cost of the second-order boundary approximation is very low. Compared with the method in Carmona and Durrleman (2005), both our methods are in closed form and only involve arithmetic calculations, thus they are quite straightforward to implement. We also extend both our methods to price hybrid spread-basket options through a technique commonly used in valuing Asian options.

Second, we consider the Greeks of the multi-asset spread option. In practical applications such as dynamic hedging and Value-at-Risk calculations, the calculation of Greeks is very important. Because the second-order boundary approximation is more accurate than the extended Kirk approximation, we use the former to compute the Greeks. We give closed-form approximations for the deltas and kappa of the multi-asset spread option in two important cases of our general framework, namely, the geometric Brownian motion case and the log–Ornstein–Uhlenbeck process case. Because the second-order boundary approximation is extremely fast and accurate, Greeks other than the deltas and kappa can be very efficiently computed using the finite difference approximation.

Finally, we perform extensive numerical experiments to study the performance of our methods and other existing methods, including Monte Carlo simulation, Carmona and Durrleman's method and numerical integration. We first perform the comparisons with different numbers of assets in the spread option, namely, 3, 20, 50 and 150 assets. Numerical integration is only performed for the three-asset case because it quickly gets inapplicable when the dimension gets higher. All results indicate that our methods are extremely fast and accurate. Between our methods, the second-order boundary approximation is a little bit slower than the extended Kirk approximation but more accurate. In particular, for the second-order boundary approximation, it takes about 3×10^{-3} s to compute the price of a spread option written on 50 underlying assets. The relative pricing error of the second-order boundary approximation is usually in the order of 10^{-4}. For the three-asset case, because computation of the Greeks using numerical integration is still feasible, we also perform a comparison of the deltas and kappa between the extended Kirk approximation and the second-order boundary approximation. We find that for the purpose of calculating Greeks, it is preferable to use the latter method. Our last comparison uses two hypothetical spread options. The first one is between the S&P 500 index and the 30 component stocks of the Dow Jones Industrial Average (DJIA) index, while the second one is between the S&P SmallCap 600 index and the DJIA components. The purpose of this experiment is to examine the performance of our methods with more realistic parameters. Also, in practice, the spreads between large company stocks and the whole market and between large and small company stocks are closely watched by industry practitioners. The results again show that our methods are fast and most accurate.

The paper is organized as follows. Section 2 discusses the general framework under which our spread option pricing results are derived, and then gives the spread option price in integration form. Section 3 develops two closed-form approximations for multi-asset spread option prices, namely, the extended Kirk approximation and the second-order boundary approximation. The implementation of the latter method is discussed in detail. We also study the Greeks of multi-asset spread options and extend both our methods to hybrid spread-basket options. Section 4 compares our methods with alternative numerical approaches and other approximations in terms of both speed and accuracy. Section 5 concludes. Proofs are given in the appendix.

2. The model setup

Consider $N+1$ assets whose prices at time t are denoted by $S_0(t), S_1(t), \ldots,$ and $S_N(t)$. We are interested in spread options with time-T payoff $[S_0(T) - \sum_{k=1}^{N} S_k(T) - K]^+$, where the strike K is a pre-specified constant. We will first assume that $K \geq 0$. Negative K cases are treated later when we discuss hybrid basket-spread options. Assuming that the interest rate r is a constant, by the martingale pricing approach, the price of a spread option Π is given by

$$\Pi = e^{-rT}\mathbb{E}^{\mathbb{Q}}\left[S_0(T) - \sum_{k=1}^{N} S_k(T) - K\right]^+, \quad (1)$$

where $\mathbb{Q}$ is the risk-neutral measure under which discounted security prices are martingales. To compute these option prices, we assume that $\log S_0(T), \log S_1(T), \ldots,$ and $\log S_N(T)$ are jointly normally distributed conditioning on the initial asset prices. Specifically, conditioning on $S_0(0) = s_0, S_1(0) = s_1, \ldots,$ and $S_N(0) = s_N$, we assume

$$\mathbb{E}^{\mathbb{Q}}[\log S_k(T)] = \mu_k, \quad \text{Var}^{\mathbb{Q}}[\log S_k(T)] = v_k^2,$$
$$k = 0, 1, \ldots, N,$$

where $\boldsymbol{\mu} \equiv \{\mu_k\}$ and $\boldsymbol{v} \equiv \{v_k\}$ are two deterministic vectors. Recasting in more familiar terms of asset returns $R_{k,T} \equiv \log(S_k(T)/s_k)$, we have

$$\mu_k = \log s_k + \mathbb{E}^{\mathbb{Q}}[R_{k,T}], \quad \text{and} \quad v_k^2 = \text{Var}^{\mathbb{Q}}[R_{k,T}],$$
$$k = 0, 1, \ldots, N. \quad (2)$$

Next, we define

$$X = \frac{\log S_0(T) - \mu_0}{v_0}, \quad Y_k = \frac{\log S_k(T) - \mu_k}{v_k},$$
$$k = 1, 2, \ldots, N. \quad (3)$$

In our setup, we will assume that X and Y_k's are jointly normally distributed with mean vector $\mathbf{0}$, variance vector $\mathbf{1}$, and the following $(N+1) \times (N+1)$ correlation matrix

$$\boldsymbol{\Sigma} = (\rho_{i,j}) = \begin{pmatrix} 1 & \boldsymbol{\Sigma}'_{10} \\ \boldsymbol{\Sigma}_{10} & \boldsymbol{\Sigma}_{11} \end{pmatrix},$$

where $\boldsymbol{\Sigma}_{10}$ is a $N \times 1$ column vector and $\boldsymbol{\Sigma}_{11}$ is the $N \times N$ correlation matrix of the Y_k's. We assume that the determinant of $\boldsymbol{\Sigma}$ is not zero. That is, the returns of the $N+1$ assets are not perfectly correlated.

This general setup incorporates two important cases, namely, the geometric Brownian motions (GBMs) case and the mean-reverting log–Ornstein–Uhlenbeck (log-OU) case. Geometric Brownian motions are frequently used to model stock prices while the log-OU processes are frequently used to model commodity prices. Specifically, let $W_k(t), k = 0, 1, \ldots, N,$ be Brownian motions with correlation matrix $\boldsymbol{\varrho} = (\varrho_{i,j})$. In the GBMs case, we have

$$dS_k = (r - q_k)S_k dt + \sigma_k S_k dW_k, \quad (4)$$

where r is the risk-free interest rate, σ_k's are the volatilities, and q_k's are the dividend rates. A simple application of Ito's lemma yields

$$\mu_k = \log s_k + (r - q_k - \sigma_k^2/2)T, \quad v_k = \sigma_k\sqrt{T}, \quad \rho_{i,j} = \varrho_{i,j}. \quad (5)$$

The GBMs case can be easily generalized to incorporate seasonality in parameters by allowing σ_k's, q_k's and $\boldsymbol{\Sigma}$ to be deterministic functions of the calendar time t. This is useful since for some spread options, their underlying assets exhibit strong seasonality in price volatilities and in their return correlations. Our general framework incorporates this generalized GBMs case.

In the log-OU case, we have

$$dS_k = -\lambda_k(\log S_k - \eta_k)S_k dt + \sigma_k S_k dW_k, \quad (6)$$

where λ_k's are the mean-reverting strength parameters and η_k's are parameters controlling the long-run means. The application of Ito's lemma now gives

$$\mu_k = \eta_k - \frac{\sigma_k^2}{2\lambda_k} + e^{-\lambda_k T}\left(\log s_k - \eta_k + \frac{\sigma_k^2}{2\lambda_k}\right),$$
$$v_k = \sigma_k\sqrt{\frac{1 - e^{-2\lambda_k T}}{2\lambda_k}}, \quad (7)$$

$$\rho_{i,j} = 2\varrho_{i,j}\frac{\sqrt{\lambda_i\lambda_j}}{\lambda_i + \lambda_j}\frac{1 - e^{-(\lambda_i + \lambda_j)T}}{\sqrt{1 - e^{-2\lambda_i T}}\sqrt{1 - e^{-2\lambda_j T}}}. \quad (8)$$

Again, with some modifications on the μ_k's, v_k's and $\boldsymbol{\Sigma}$, our general framework can incorporate the log-OU case with time-varying parameters.

Before introducing our methods for computing the spread option price, we present an analysis of the exercise boundary. At time T, the spread option is in-the-money if $S_0(T) - \sum_{k=1}^{N} S_k(T) - K \geq 0$. If $K \geq 0$, this condition is the same as

$$X \geq \frac{\log(\sum_{k=1}^{N} e^{v_k Y_k + \mu_k} + K) - \mu_0}{v_0}.$$

Thus, conditioning on $Y_k = y_k$, the option is in-the-money if $X \geq \underline{x}(\mathbf{y})$, where

$$\underline{x}(\mathbf{y}) \equiv \frac{\log(\sum_{k=1}^{N} e^{v_k y_k + \mu_k} + K) - \mu_0}{v_0}. \tag{9}$$

Notice that since $K \geq 0$, equation (9) is always binding since the right-hand side is a finite real number. Also notice that $\underline{x}(\mathbf{y})$ is a nonlinear function in the components of $\mathbf{y}$.

Throughout the paper, we use $\phi(\mathbf{z}; \mathbf{m}, \Sigma)$ to stand for the multivariate normal density function with mean vector $\mathbf{m}$ and covariance matrix Σ, and $\Phi(z)$ for the one-dimensional cumulative normal distribution function. If $\mathbf{m}$ and Σ are scalers with $\mathbf{m} = 0$, and $\Sigma = 1$, we will simply write $\phi(z)$ for $\phi(z; 0, 1)$. Notice that the random variables X and Y in equation (3) are jointly normally distributed with density $\phi(\{x, \mathbf{y}\}; \mathbf{0}, \Sigma)$. By risk-neutral valuation, the computation of spread option price Π involves an $(N+1)$-dimensional integration as follows:

$$\Pi = \Pi(\boldsymbol{\mu}, \mathbf{v}, \Sigma) = e^{-rT} \int_{\mathbb{R}^N} \int_{\mathbb{R}} \left(e^{v_0 x + \mu_0} - \sum_{k=1}^{N} e^{v_k y_k + \mu_k} - K \right)^+$$
$$\times \phi(\{x, \mathbf{y}\}; \mathbf{0}, \Sigma) \, dx \, d\mathbf{y}. \tag{10}$$

However, in the following proposition, we reduce the above integral to $N + 2$ N-dimensional integrations based on a technique in Pearson (1995).

Proposition 2.1: *Under the jointly-normal returns setup with $K \geq 0$ and det $\Sigma \neq 0$, the price of the spread option can be written as*

$$\Pi = e^{-rT + \mu_0 + \frac{1}{2}v_0^2} \mathbf{I}_0 - \sum_{k=1}^{N} e^{-rT + \mu_k + \frac{1}{2}v_k^2} \mathbf{I}_k - Ke^{-rT} \mathbf{I}_{N+1}. \tag{11}$$

The integrals $\mathbf{I}_i$'s are given by

$$\mathbf{I}_0 = \int_{\mathbb{R}^N} \phi(\mathbf{y}; \mathbf{0}, \Sigma_{11}) \, \Phi\left(A(\mathbf{y} + v_0 \Sigma_{10}) + v_0 \sqrt{\Sigma_{x|\mathbf{y}}} \right) d\mathbf{y}, \tag{12}$$

$$\mathbf{I}_k = \int_{\mathbb{R}^N} \phi(\mathbf{y}; \mathbf{0}, \Sigma_{11}) \, \Phi\left(A(\mathbf{y} + v_k \Sigma_{11} \mathbf{e}_k) \right) d\mathbf{y}, \tag{13}$$
$$k = 1, 2, \ldots, N$$

$$\mathbf{I}_{N+1} = \int_{\mathbb{R}^N} \phi(\mathbf{y}; \mathbf{0}, \Sigma_{11}) \, \Phi\left(A(\mathbf{y}) \right) d\mathbf{y}, \tag{14}$$

where $\mathbf{e}_k$ is the unit column vector $(0, \ldots, 0, 1, 0, \ldots, 0)'$ with 1 at the kth position, and

$$A(\mathbf{y}) = \frac{\mu_{x|\mathbf{y}} - \underline{x}(\mathbf{y})}{\sqrt{\Sigma_{x|\mathbf{y}}}}, \tag{15}$$

with

$$\mu_{x|\mathbf{y}} = \Sigma_{10}' \Sigma_{11}^{-1} \mathbf{y}, \quad \Sigma_{x|\mathbf{y}} = 1 - \Sigma_{10}' \Sigma_{11}^{-1} \Sigma_{10}. \tag{16}$$

Notice that when det $\Sigma \neq 0$, we have $\Sigma_{x|\mathbf{y}} \neq 0$ and det $\Sigma_{11} \neq 0$, so $A(\mathbf{y})$ is always well-defined. Also, notice that in the geometric Brownian motions case, the price Π

reduces to the more familiar form

$$\Pi = s_0 e^{-q_0 T} \mathbf{I}_0 - \sum_{k=1}^{N} s_k e^{-q_k T} \mathbf{I}_k - Ke^{-rT} \mathbf{I}_{N+1}.$$

Proposition 2.1 gives a formula for the spread option price which resembles the Black–Scholes formula (Black and Scholes 1973). In particular, the price of the spread option Π in equation (11) consists of three terms. The first term is the present value of the risk-neutral expected future benefit of receiving asset S_0. The second term is the present value of expected future cost of giving up assets S_k, where $k = 1, \ldots, N$. The last term is the present value of the expected cost of giving up an additional monetary amount K. The quantities $A(\mathbf{y})$ and $\mathbf{I}_i$'s also have intuitive meanings. The quantity $A(\mathbf{y})$ is the *conditional moneyness* of the spread option because $A(\mathbf{y})$ plays a similar role as d_2 in the Black–Scholes formula. This can be seen from the proof of Proposition 2.1 that the quantity $\Phi(A(\mathbf{y}))$ is the risk-neutral probability that the spread option expires in the money conditioning on that the vector of standardized log prices of assets $\{S_k\}$ is $\mathbf{y}$. Written out explicitly, we have

$$\Phi(A(\mathbf{y})) = \text{Prob}^{\mathbb{Q}} \Bigg[S_0(T) \geq \sum_{k=1}^{N} S_k(T) + K \, \Bigg|$$
$$Y_k \equiv \frac{\log S_k(T) - \mu_k}{v_k} = y_k,$$
$$k = 1, \ldots, N \Bigg]. \tag{17}$$

Similar to the Black–Scholes formula, the quantity $\mathbf{I}_{N+1}$ is the unconditional probability that the spread option will expire in the money under the risk-neutral distribution. The proof of Proposition 2.1 shows that $\mathbf{I}_0$ and $\mathbf{I}_k$ have similar meanings as $\mathbf{I}_{N+1}$. They are the probabilities that the spread option will expire in the money under the measures in which asset S_0 and S_k are taken to be the numeraire asset, respectively. This is similar to the case of the Black–Scholes formula, where the term $\Phi(d_1)$ is the probability that the option will expire in the money under the probability measure in which the underlying stock is taken as the numeraire asset.

The proof of Proposition 2.1 is given in the appendix. Proposition 2.1 highlights the importance of the exercise boundary and is the starting point of our approximation. Our goal now is to approximate $A(\mathbf{y})$ so that the $\mathbf{I}_k$'s can be performed in closed form. In the next section, we give two closed-form approximations for computing the spread option price Π.

3. Closed-form approximations

3.1. Extended Kirk approximation

Kirk (1995) gives a fairly accurate closed-form approximation for two-asset spread option prices. Li *et al.* (2008) compare its performance with other methods and point out that Kirk's formula can be obtained by a linear

approximation of the exercise boundary. In this subsection, we extend Kirk's approximation to a multi-asset setting. Our idea is to first approximate $\sum_{k=1}^{N} S_k(T)$ as a lognormal random variable and then apply Kirk's approximation for two-asset spread options. This can be achieved by approximating $\sum_{k=1}^{N} S_k(T)/N$ by the corresponding geometric average $(\prod_{k=1}^{N} S_k(T))^{1/N}$, a technique commonly used in pricing Asian options. The result is the following.

Proposition 3.1: *Under the general jointly-normal returns setup, the multi-asset spread option price can be approximated as*

$$\Pi \approx e^{-rT+\mu_0+\frac{1}{2}v_0^2} \Phi\left(d_K + \frac{v_K}{2}\right)$$
$$- \left(\sum_{k=1}^{N} e^{-rT+\mu_k+\frac{1}{2}v_k^2} + Ke^{-rT}\right) \Phi\left(d_K - \frac{v_K}{2}\right), \quad (18)$$

where

$$v_K = \sqrt{v_0^2 - 2\rho_a v_0 v_a m + v_a^2 m^2}, \quad d_K = \frac{\log m_0}{v_K},$$

with

$$m_0 = \frac{e^{\mu_0+\frac{1}{2}v_0^2}}{\sum_{k=1}^{N} e^{\mu_k+\frac{1}{2}v_k^2} + K}, \quad m = \frac{\sum_{k=1}^{N} e^{\mu_k+\frac{1}{2}v_k^2}}{\sum_{k=1}^{N} e^{\mu_k+\frac{1}{2}v_k^2} + K},$$
$$v_a = \frac{1}{N}\sqrt{\sum_{i=1}^{N}\sum_{j=1}^{N} \rho_{i,j} v_i v_j}, \quad \rho_a = \frac{1}{Nv_a}\left(\sum_{k=1}^{N} \rho_{0,k} v_k\right).$$

The proof of the above proposition is given in the appendix. Notice that the above proposition works for all models in our general jointly normal returns setup, in particular, for the GBMs and the log-OU case. In the GBMs case, equation (18) becomes

$$\Pi \approx s_0 e^{-q_0 T} \Phi\left(d_K + \frac{v_K}{2}\right)$$
$$- \left(\sum_{k=1}^{N} s_k e^{-q_k T} + Ke^{-rT}\right) \Phi\left(d_K - \frac{v_K}{2}\right), \quad (19)$$

and resembles the Black–Scholes formula or more closely, the Margrabe (1978) formula. The extended Kirk approximation is extremely easy to implement and extremely fast. Another advantage of the above approximation is that it also works when det Σ is very close to 0.

Numerical experiments in section 4 show that the extended Kirk approximation is most accurate when the $S_k(T)$'s $(k=1,\ldots,N)$ are more symmetric. That is, the $\rho_{i,j}$'s are about the same, initial asset prices s_i's are about the same, and μ_i's and v_i's are about the same. The reason is that in this case, the geometric average of the $S_k(T)$ is closer to the arithmetic average. We also conduct an experiment where the $S_k(T)$'s $(k=1,\ldots,N)$ are not very symmetric using a hypothetical spread option between the S&P 500 Index and the 30 component stocks of the Dow Jones Industrial Average Index. We see that when the assets are not very symmetric, the extended Kirk approximation is not as accurate as the second-order

boundary approximation which we are introducing below. Also, by the nature of its design, the extended Kirk approximation does not give as accurate Greeks as the second-order boundary approximation does.

3.2. Second-order boundary approximation

As Li *et al.* (2008) point out, one will obtain Kirk's approximation if one uses linear approximations to approximate the conditional moneyness function $A(\mathbf{y})$. Li *et al.* (2008) derive an approximation for two-asset spread options based on a second-order approximation of the exercise boundary. They also show that when the curvature of the exercise boundary is not large, the second-order boundary approximation is extremely efficient and more accurate than existing methods such as Kirk's approximation. It turns out that their method could be generalized to arbitrary number of assets. Below we give the generalized results for multi-asset spread options.

Two observations of Proposition 2.1 are very useful. First, the integrals $\mathbf{I}_i$'s all involve $\phi(\mathbf{y}; \mathbf{0}, \Sigma_{11})$ which is quite peaked around $\mathbf{y}=\mathbf{0}$. Second, around $\mathbf{y}=\mathbf{0}$, the exercise boundary $\underline{x}(\mathbf{y})$ is quite close to being linear in $\mathbf{y}$. Hence the same is true for the function $A(\mathbf{y})$. Figure 1 confirms this by giving a sample plot of $A(\mathbf{y})$ when $N=2$. The parameters used are the same ones we use later for numerical comparisons in the three-asset case, and we fix $K=30$ with $\sigma_i=0.3$ for all three assets.

We now derive the approximations for the exercise boundary $\underline{x}(\mathbf{y})$ of the spread option and the function $A(\mathbf{y})$ to second order in $\mathbf{y}$ around $\mathbf{y}=\mathbf{0}$ as follows:

Proposition 3.2: *The exercise boundary $\underline{x}(\mathbf{y})$ can be approximated to second order in $\mathbf{y}$ as*

$$\underline{x}(\mathbf{y}) \approx \underline{x}(\mathbf{0}) + \nabla\underline{x}|_{\mathbf{0}}' \, \mathbf{y} + \frac{1}{2}\mathbf{y}'\nabla^2\underline{x}|_{\mathbf{0}} \, \mathbf{y},$$
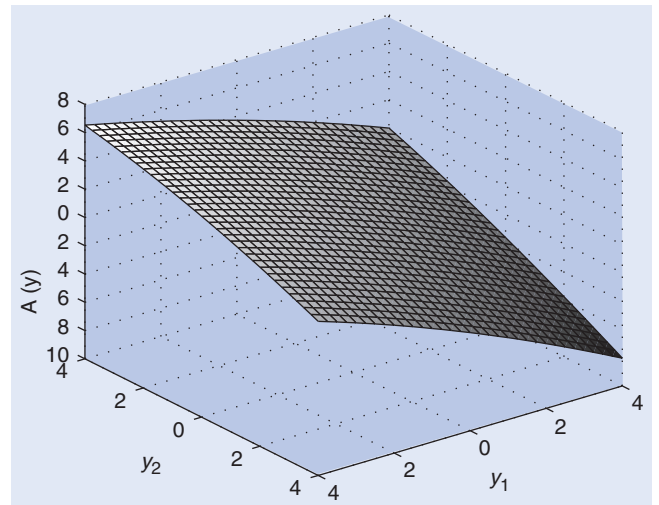

Figure 1. The function $A(\mathbf{y})$ near $\mathbf{y}=\mathbf{0}$. Notice that $A(\mathbf{y})$ is approximately linear in $\mathbf{y}$ around $\mathbf{y}=\mathbf{0}$, with some modest curvature.

where

$$\underline{x}(\mathbf{0}) = \frac{\log(R+K) - \mu_0}{\nu_0},$$

$$(\nabla\underline{x}|_{\mathbf{0}})_k = \frac{e^{\mu_k}\nu_k}{\nu_0(R+K)}, \quad k = 1, 2, \dots, N,$$

$$(\nabla^2\underline{x}|_{\mathbf{0}})_{i,j} = -\frac{\nu_i\nu_j e^{\mu_i+\mu_j}}{\nu_0(R+K)^2} + \delta_{i,j}\frac{\nu_j^2 e^{\mu_j}}{\nu_0(R+K)}, \quad i,j = 1,2,\dots$$

with $\delta_{i,j}$ being the Kronecker delta function, and

$$R = \sum_{k=1}^N e^{\mu_k}.$$

Accordingly, the function $A(\mathbf{y})$ can be approximated as

$$A(\mathbf{y}) = \frac{\mu_{x|\mathbf{y}} - \underline{x}(\mathbf{y})}{\sqrt{\Sigma_{x|\mathbf{y}}}} \approx c + \mathbf{d}'\mathbf{y} + \mathbf{y}'\mathbf{E}\mathbf{y},$$

where

$$c = -\frac{\log(R+K) - \mu_0}{\nu_0\sqrt{\Sigma_{x|\mathbf{y}}}}, \tag{20}$$

$$\mathbf{d} = \frac{1}{\sqrt{\Sigma_{x|\mathbf{y}}}}(\Sigma_{11}^{-1}\Sigma_{10} - \nabla\underline{x}|_{\mathbf{0}}), \tag{21}$$

$$\mathbf{E} = -\frac{1}{2\sqrt{\Sigma_{x|\mathbf{y}}}}(\nabla^2\underline{x}|_{\mathbf{0}}). \tag{22}$$

Our goal is to use an approximation of $A(\mathbf{y})$ in Proposition 2.1 so that we can perform the integrals I_k's. For this purpose, we further expand $\Phi(c + \mathbf{d}'\mathbf{y} + \mathbf{y}'\mathbf{E}\mathbf{y})$ into three terms to second order in $\mathbf{y}'\mathbf{E}\mathbf{y}$ around $\mathbf{y}'\mathbf{E}\mathbf{y} = \epsilon$, for some suitably chosen ϵ. Intuitively, we should choose ϵ to be the unconditional mean of $Y'EY$, which is given by the trace of the matrix $\mathbf{F}$ below. With the help of an identity in Li (2008), we are now able to perform the integration and obtain a closed-form approximation for the spread option price as presented in Proposition 3.3. Proposition 3.3 is one of the most important results of this paper. The proof of Proposition 3.3 is given in the appendix.

Proposition 3.3: *Let $K \geq 0$ and $det\,\Sigma \neq 0$. The spread option price Π under the general jointly-normal returns setup is given by*

$$\Pi = e^{-rT+\mu_0+\frac{1}{2}\nu_0^2}\mathbf{I}_0 - \sum_{k=1}^N e^{-rT+\mu_k+\frac{1}{2}\nu_k^2}\mathbf{I}_k - Ke^{-rT}\,\mathbf{I}_{N+1}. \tag{23}$$

The integrals $\mathbf{I}_i$'s are approximated as

$$\mathbf{I}_i \approx \mathbf{J}^0(c_i, \mathbf{d}_i) + \mathbf{J}^1(c_i, \mathbf{d}_i) - \frac{1}{2}\mathbf{J}^2(c_i, \mathbf{d}_i), \quad i = 0, 1, \dots, N+1, \tag{24}$$

where the scaler function $\mathbf{J}^i$'s are defined as

$$\mathbf{J}^0(u, \mathbf{v}) = \Phi\left(\frac{u}{\sqrt{1+\mathbf{v}'\mathbf{v}}}\right), \tag{25}$$

$$\mathbf{J}^1(u, \mathbf{v}) = \frac{\lambda}{\sqrt{1+\mathbf{v}'\mathbf{v}}} \cdot \phi\left(\frac{u}{\sqrt{1+\mathbf{v}'\mathbf{v}}}\right), \tag{26}$$

$$\mathbf{J}^2(u, \mathbf{v}) = \frac{u}{(1+\mathbf{v}'\mathbf{v})^{3/2}} \cdot \phi\left(\frac{u}{\sqrt{1+\mathbf{v}'\mathbf{v}}}\right)$$
$$\left\{\lambda^2 + 2tr[(\mathbf{PFP})^2] - 4\lambda(1+\mathbf{v}'\mathbf{v})(\mathbf{v}'\mathbf{P}^2\mathbf{FP}^2\mathbf{v})\right.$$
$$\left. + (4u^2 - 8 - 8\mathbf{v}'\mathbf{v})\|\mathbf{PFP}^2\mathbf{v}\|^2\right\}, \tag{27}$$

with

$$\mathbf{P} = \mathbf{P}(\mathbf{v}) \equiv (\mathbf{I} + \mathbf{v}\mathbf{v}')^{-1/2}, \tag{28}$$

$$\lambda = \lambda(u, \mathbf{v}) \equiv u^2\mathbf{v}'\mathbf{P}^2\mathbf{FP}^2\mathbf{v} + tr(\mathbf{PFP}) - tr(\mathbf{F}), \tag{29}$$

where tr stands for the trace operator of a matrix. The scalers c_i, vectors $\mathbf{d}_i$, and matrix $\mathbf{F}$ are given by

$$c_0 = c + tr(\mathbf{F}) + \nu_0\sqrt{\Sigma_{x|\mathbf{y}}} + \nu_0\Sigma_{10}'\mathbf{d} + \nu_0^2\Sigma_{10}'\mathbf{E}\Sigma_{10}, \tag{30}$$

$$\mathbf{d}_0 = \Sigma_{11}^{1/2}(\mathbf{d} + 2\nu_0\mathbf{E}\Sigma_{10}), \tag{31}$$

$$c_k = c + tr(\mathbf{F}) + \nu_k\mathbf{e}_k'\Sigma_{11}\mathbf{d} + \nu_k^2\mathbf{e}_k'\Sigma_{11}\mathbf{E}\Sigma_{11}\mathbf{e}_k,$$
$$k = 1, 2, \dots, N, \tag{32}$$

$$\mathbf{d}_k = \Sigma_{11}^{1/2}(\mathbf{d} + 2\nu_k\mathbf{E}\Sigma_{11}\mathbf{e}_k), \quad k = 1, 2, \dots, N, \tag{33}$$

$$c_{N+1} = c + tr(\mathbf{F}), \tag{34}$$

$$\mathbf{d}_{N+1} = \Sigma_{11}^{1/2}\mathbf{d}, \tag{35}$$

$$\mathbf{F} = \Sigma_{11}^{1/2}\mathbf{E}\Sigma_{11}^{1/2}, \tag{36}$$

with $\Sigma_{x|\mathbf{y}}$ given in Proposition 2.1 and c, $\mathbf{d}$, $\mathbf{E}$ given in Proposition 3.2.

Notice that we have used boldface subscript i in $\mathbf{d}_i$ to denote the ith vector in order to avoid confusion with the ith component $\mathbf{d}_i$ of the vector $\mathbf{d}$. That is, each $\mathbf{d}_i$ is a vector, and we have $N+2$ of them, for $i = 0, 1, \dots, N+1$. As we see, the calculation of the spread option price is quite straightforward in the second-order boundary approximation. If one is not too concerned with accuracy, one could omit the $\mathbf{J}^2$'s in the approximation, which we call the first-order boundary approximation.

A naive look at Proposition 3.3 might imply that we need to perform a lot of costly matrix multiplications. However, Proposition 3.4 below shows that we only need to perform a very limited number of matrix multiplications. The critical observation in obtaining Proposition 3.4 is that $\mathbf{v}$ is an eigenvector of $\mathbf{P}(\mathbf{v})$ defined in equation (28). The proof of Proposition 3.4 is given in the appendix.

Proposition 3.4: *With $\mathbf{P} = \mathbf{P}(\mathbf{v})$ as defined in equation (28), we have*

$$\mathbf{P} = \mathbf{I} - \theta\mathbf{v}\mathbf{v}', \quad \mathbf{P}^2 = \mathbf{I} - \psi\mathbf{v}\mathbf{v}',$$

where the scalars θ and ψ are given by

$$\theta = \theta(\mathbf{v}) = \frac{\sqrt{1 + \mathbf{v}'\mathbf{v}} - 1}{\mathbf{v}'\mathbf{v}\sqrt{1 + \mathbf{v}'\mathbf{v}}}, \quad \psi = \psi(\mathbf{v}) = \frac{1}{1 + \mathbf{v}'\mathbf{v}}. \quad (37)$$

Furthermore, we have

$$tr[(\mathbf{PFP})^2] = tr(\mathbf{F}^2) - \psi(1 + \psi)\mathbf{v}'\mathbf{F}^2\mathbf{v}, \quad (38)$$

$$\mathbf{v}'\mathbf{P}^2\mathbf{F}\mathbf{P}^2\mathbf{v} = \psi^2\mathbf{v}'\mathbf{F}\mathbf{v}, \quad (39)$$

$$\|\mathbf{PFP}^2\mathbf{v}\|^2 = \psi^2[\mathbf{v}'\mathbf{F}^2\mathbf{v} - \psi(\mathbf{v}'\mathbf{F}\mathbf{v})^2], \quad (40)$$

$$tr(\mathbf{PFP}) = tr(\mathbf{F}) - \psi\mathbf{v}'\mathbf{F}\mathbf{v}. \quad (41)$$

Thus the scaler function $\mathbf{J}^i$'s given in (25) can be simplified as

$$\mathbf{J}^0(u, \mathbf{v}) = \Phi\left(u\sqrt{\psi}\right), \quad (42)$$

$$\mathbf{J}^1(u, \mathbf{v}) = \psi^{3/2}(\psi u^2 - 1)\mathbf{v}'\mathbf{F}\mathbf{v} \cdot \phi\left(u\sqrt{\psi}\right), \quad (43)$$

$$\mathbf{J}^2(u, \mathbf{v}) = u\psi^{3/2} \cdot \phi\left(u\sqrt{\psi}\right)$$
$$\times \left\{ 2tr(\mathbf{F}^2) - 4(1 - tr(\mathbf{F}))(\psi - \psi^2)\mathbf{v}'\mathbf{F}\mathbf{v} \right.$$
$$+ \psi^2(9 + (2 - 3u^2)\psi - u^2(4 - u^2)\psi^2)(\mathbf{v}'\mathbf{F}\mathbf{v})^2$$
$$\left. - 2\psi(5 + (1 - 2u^2)\psi)\mathbf{v}'\mathbf{F}^2\mathbf{v} \right\}. \quad (44)$$

Proposition 3.4 is very useful in the actual implementation of the second-order boundary approximation because it reduces the calculation of the four computationally costly terms in Proposition 3.3, $tr[(\mathbf{PFP})^2]$, $\mathbf{v}'\mathbf{P}^2\mathbf{F}\mathbf{P}^2\mathbf{v}$, $\|\mathbf{PFP}^2\mathbf{v}\|^2$ and $tr(\mathbf{PFP})$, to four much simpler expressions, namely, $tr(\mathbf{F})$, $tr(\mathbf{F}^2)$, $\mathbf{v}'\mathbf{F}\mathbf{v}$, and $\mathbf{v}'\mathbf{F}^2\mathbf{v}$. Our numerical analysis shows that Proposition 3.4 reduces the computational time of the second-order boundary approximation as presented in Proposition 3.3 by about several hundred times for relatively large N. The larger the N, the more important it is to use Proposition 3.4. In the appendix we comment more on the efficient implementation of the second-order boundary approximation. When $N = 1$ so that we are dealing with two-asset spread options, $\mathbf{v}$'s are all scalars and so are $\mathbf{P}$ and $\mathbf{F}$. In this case, we could use either Proposition 3.3 or Proposition 3.4.

It is worthwhile emphasizing that in addition to being applicable to spread options with arbitrary number of assets, the second-order boundary approximation above in this paper is also more accurate than the one in Li *et al.* (2008) when specialized to the case of two-asset spread options. The mathematical reason is that in developing Proposition 3.3, we have changed the expansion point for the second-order boundary approximation. For two-asset spread options, $\mathbf{E}$ (denoted as ϵ by Li *et al.*) and y are both scalars. In Li *et al.* (2008), the expansion point is chosen to be $\epsilon y^2 = 0$, while in this paper we have chosen the expansion point to be $\epsilon y^2 = \epsilon$. Intuitively, the new expansion point works much better because the mean of y^2 is 1, so we are expanding around the mean. Later we

will compare the performance of the second-order boundary approximation with other existing methods.

Proposition 3.3 gives an approximation for the multi-asset spread option price but does not provide an error estimate. There are a few approaches to deal with the error estimate. First, Li *et al.* (2008) provide lower and upper bounds for the digital spread options in the two-asset spread option case. Although the algebra would be much more complicated, it is possible to generalize these bounds to the multi-asset spread option case. Second, as long as the nonlinearity in $A(\mathbf{y})$ is relatively mild, the approximation method in this paper is convergent in that if we keep more and more higher-order terms, then the approximating option prices will approach the true price (see the remarks in the proof of Proposition 3.3). In this paper, we have only kept the lowest two orders. It is possible to get an estimate (or lower and upper bounds) for the third-order term, which takes into account the higher-order nonlinearity in the conditional moneyness $A(\mathbf{y})$. Third, as we will see in our numerical analysis, the second-order approximation is extremely accurate when compared to Monte Carlo estimates of the true prices. The absolute difference between the Monte Carlo price and the second-order boundary approximation when added to the standard error of the Monte Carlo approximation could be used as an estimate for the approximation error of the second-order boundary approximation. Finally, as an operationally extremely simple but relatively conservative method, we could simply use the difference between the first-order and second-order boundary approximations as the error bound for the second-order boundary approximation.

In the next subsection, we consider the Greeks of the spread options.

3.3. Spread option Greeks and their approximation

Propositions 3.1 and 3.3 give approximations for multi-asset spread options prices. Below we derive approximations for the important Greeks in our setup. Fast and accurate calculation of these Greeks is very important because the Greeks are very useful in hedging, portfolio rebalancing, risk assessment such as VaR calculations, among other things. There are many approaches to calculating the Greeks, including finite difference method using Monte Carlo, numerical integration, and more recently, Malliavin calculus. For multi-asset spread options, especially when the number of assets is large, numerical methods often prove to be extremely slow to be applicable in practice. Thus a closed-form approximation is extremely useful. We use the second-order boundary approximation in the computation of the Greeks because although the extended Kirk approximation is fairly accurate for the prices, it does not give as accurate Greeks as the second-order boundary approximation does.

We will focus on the most important Greeks, the deltas and kappa. Because the second-order boundary approximation is extremely fast and accurate, Greeks other than the deltas and kappa can be very efficiently computed using the finite difference method.

To compute the deltas and kappa, we need to know the dependence of μ_k's and ν_k's on the initial asset prices s_k's and the strike price K. We will assume that for each k, μ_k is a function of s_k while ν_k is independent of s_k. This is not very restrictive because both the two important special cases of our general setup, namely, the GBMs case and the log-OU case, satisfy this requirement.

Now let us define the price vector

$$\mathbf{S} = (e^{-rT+\mu_0+\frac{1}{2}v_0^2}, -e^{-rT+\mu_1+\frac{1}{2}v_1^2}, \ldots, -e^{-rT+\mu_N+\frac{1}{2}v_N^2}, -Ke^{-rT})'.$$

Be careful with the minus signs in the above definition. This definition allows us to write the spread option price formally as $\Pi = \mathbf{S}'\mathbf{I}$. Notice that in the GBMs case, equation (5) holds so

$$\mathbf{S} = (s_0 e^{-q_0 T}, -s_1 e^{-q_1 T}, \ldots, -s_N e^{-q_N T}, -Ke^{-rT}). \quad (45)$$

In the log-OU case, equation (7) gives us that for $k = 0, 1, \ldots, N$,

$$\begin{aligned}
\mathbf{S}_k &= (1_{k=0} - 1_{k>0}) \\
&\times \exp\Big(-rT + \eta_k(1 - e^{-\lambda_k T}) \\
&\quad + e^{-\lambda_k T}\log s_k - \frac{\sigma_k^2}{4\lambda_k}\big(1 - e^{-\lambda_k T}\big)^2 \Big).
\end{aligned} \quad (46)$$

From Proposition 2.1 and 3.3, we have the following result for the deltas and kappa. The proof of Proposition 3.5 is in the appendix.

Proposition 3.5: *Let $K \geq 0$. Suppose that in the general jointly normal returns setup, μ_k is only a function of s_k while ν_k is independent of s_k for each $k = 1, \ldots, N$. Then*

$$\Delta_0 \equiv \frac{\partial \Pi}{\partial s_0} = \frac{\partial \mu_0}{\partial s_0}\mathbf{S}_0\mathbf{I}_0, \quad (47)$$

$$\Delta_k \equiv \frac{\partial \Pi}{\partial s_k} = -\frac{\partial \mu_k}{\partial s_k}|\mathbf{S}_k|\mathbf{I}_k, \quad k = 1, 2, \ldots, N, \quad (48)$$

$$\kappa \equiv \frac{\partial \Pi}{\partial K} = -e^{-rT}\mathbf{I}_{N+1}. \quad (49)$$

In particular, in the geometric Brownian motions case, we have

$$\Delta_0 = e^{-q_0 T}\mathbf{I}_0, \quad \Delta_k = -e^{-q_k T}\mathbf{I}_k, \quad k = 1, 2, \ldots, N.$$

In the log–Ornstein–Uhlenbeck case, with $\mathbf{S}_k$'s given in equation (46), we have

$$\Delta_0 = \frac{e^{-\lambda_0 T}}{s_0}\mathbf{S}_0\mathbf{I}_0, \quad \Delta_k = -\frac{e^{-\lambda_k T}}{s_k}|\mathbf{S}_k|\mathbf{I}_k, \quad k = 1, 2, \ldots, N.$$

The vector $\mathbf{I} = \{\mathbf{I}_k\}$ can then be approximated by Proposition 3.3.

Proposition 3.5 shows that Proposition 3.3 is not only useful for computing spread option prices, but also useful for computing the deltas and kappa of the spread option. In particular, if Proposition 3.3 is implemented with the vectorization technique, then the computation of the vector $\mathbf{I}$ simultaneously gives us all the deltas and kappa. This is not the case if one uses Monte Carlo simulation to

compute the prices and then uses finite difference to approximate the Greeks.

3.4. Extension to hybrid spread-basket option prices

We now extend both the extended Kirk approximation and the second-order boundary approximation to a generic hybrid spread-basket option with time-T payoff

$$\left[\sum_{i=1}^{M} w_i S_i(T) - \sum_{j=M+1}^{M+N} w_j S_j(T) - K\right]^+,$$

where K, w_i's are positive constants. Again, we assume that conditioning on the initial asset prices, $\log S_i(T)$ are jointly normally distributed with mean μ_i, variance v_i^2, and correlation matrix $(\rho_{i,j})$ for $i,j = 1, 2, \ldots, M+N$. Without loss of generality, we will assume that all w_i equal 1 as the weights w_i can be easily absorbed by defining $\widetilde{S}_i = w_i S_i$ and noticing that $\widetilde{\mu}_i = \log w_i + \mu_i$, $\widetilde{v}_i = v_i$ and $\widetilde{\rho}_{i,j} = \rho_{i,j}$. In addition, we allow one of S_i $(i = 1, \ldots, M)$ to be a constant, thus effectively allowing K to be negative. Except for the possibility of a constant S_i for some i, we assume the correlation matrix of $\log S_i$'s is positive definite.

To compute the price of this hybrid spread-basket option, we again utilize the well-known technique in pricing Asian options. Specifically, let

$$H_0(t) \equiv \sum_{i=1}^{M} S_i(t), \quad \text{and} \quad H_k(t) \equiv S_{k+M}(t) \quad k = 1, 2, \ldots, N.$$

Notice that the final payoff of the hybrid option now formally reduces to that of a standard spread option

$$\left[H_0(T) - \sum_{k=1}^{N} H_k(T) - K\right]^+.$$

However, the H_i's are no longer jointly normally distributed, nor is $H_0(T)$ normally distributed. The idea is to approximate the distribution of $H_0(T)$ by the corresponding geometric average of the S_i's. In addition, in order to apply Proposition 3.3, we need the correlation matrix of the H_i's. The detailed procedure is as follows.

Define random variables X and Y_k's by

$$X = \frac{\log H_0(T) - \mu_0^H}{v_0^H}, \quad Y_k = \frac{\log H_k(T) - \mu_k^H}{v_k^H},$$

$$k = 1, 2, \ldots, N$$

with $\mu_k^H = \mu_{k+M}$ and $v_k^H = v_{k+M}$ for $k = 1, \ldots, N$, and

$$\mu_0^H = \log\left(\sum_{i=1}^{M} e^{\mu_i + \frac{1}{2}v_i^2}\right) - \frac{1}{2}(v_0^H)^2,$$

$$v_0^H = \frac{1}{M}\sqrt{\sum_{i=1}^{M}\sum_{j=1}^{M} \rho_{i,j} v_i v_j}.$$

Then X and the Y_i's can be approximated as jointly normally distributed with mean vector $\mathbf{0}$, variance

vector **1**, and correlation matrix $\boldsymbol{\Sigma} = (\varrho_{i,j})$, $i,j = 0, 1, \ldots, N$, where

$$\varrho_{0,0} = 1,$$

$$\varrho_{0,k} = \varrho_{k,0} = \frac{1}{M\nu_0^H}\left(\sum_{i=1}^{M} \rho_{i,k}\nu_i\right), \quad k = 1, 2, \ldots, N,$$

$$\varrho_{i,j} = \rho_{M+i,M+j}, \quad i,j = 1, 2, \ldots, N.$$

The above equations can be proven in a very similar way to Proposition 3.1. Notice that under the GBMs case, the quantity μ_0^H are usually further approximated as

$$\mu_0^H = \log H_0(0) + \left(rT - \frac{1}{M}\sum_{i=1}^{M} q_i T - \frac{1}{2M}\sum_{i=1}^{M}\nu_i^2\right).$$

Once we have approximated the H_i's using the jointly normal setup, we can use either the extended Kirk approximation in Proposition 3.1 or the second-order boundary approximation in Proposition 3.3 to compute the price of the hybrid spread-basket option. This extension to hybrid spread-basket options greatly enhances the applicability of our approximation methods.

4. Comparison of accuracy and speed with existing methods

4.1. Existing pricing methods

When the number of assets is small, the numerical integration method can be used to calculate spread option prices by using Proposition 2.1. Although very accurate, it is not quite applicable for multi-asset spread options when the number of assets is large because of the huge computation cost. The same is true for the partial differential equation technique. Another widely used numerical method is Monte Carlo simulation. The advantage of Monte Carlo simulation is that it is very flexible and is able to value spread options under many different distributional assumptions. The shortcomings are as follows. First, the results from Monte Carlo are not always accurate enough, even after variance reduction techniques, such as the antithetic method, control variate and importance sampling are applied. Second, the Greeks usually need to be calculated with extra effort, usually by approximating them using finite difference. Finally, the biggest shortcoming is that Monte Carlo simulation is generally very time-consuming, especially when the dimension is high and the number of option prices need to be computed is large.

Given the high computational cost of numerical methods for the multi-asset spread option, it is extremely useful to design approximation techniques. However, until very recently, not much work has been done on this subject. Carmona and Durrleman (2005) propose approximate formulas for the lower and upper bounds of multi-asset spread options by solving a nonlinear optimization problem. They only consider the geometric Brownian motions case. The lower bound is quite accurate while the upper bound is less accurate. Therefore we just compare our method with their lower bound. We give a brief description of the Carmona and Durrleman method below. Interpreting $\sigma_{N+1} = 0$ and letting $\mathbf{C} = \boldsymbol{\Sigma} \oplus 1$ (the direct sum of $\boldsymbol{\Sigma}$ with the scaler 1), the lower bound of the spread option price is given as follows:

$$\Pi = \sum_{i=0}^{N+1} \mathbf{S}_i \Phi\left(d^* + (\mathbf{C}^{1/2}\mathbf{z}^*)_i \sigma_i \sqrt{T}\right),$$

where the scaler d^* and unit-length vector $\mathbf{z}^*$ satisfy the following system of nonlinear equations

$$\sum_{i=0}^{N+1} \mathbf{S}_i\sigma_i\sqrt{T}(\mathbf{C}^{1/2})_{ij}\ \phi\left(d^* + (\mathbf{C}^{1/2}\mathbf{z}^*)_i\sigma_i\sqrt{T}\right) - \mu z_j^* = 0,$$
$$\text{for } j = 0, \ldots, N+1, \tag{50}$$

$$\sum_{i=0}^{N+1} \mathbf{S}_i\ \phi\left(d^* + (\mathbf{C}^{1/2}\mathbf{z}^*)_i\sigma_i\sqrt{T}\right) = 0, \tag{51}$$

and μ is the Lagrangian multiplier. Notice that Carmona and Durrleman's method is not in closed form because it requires the numerical solution of a system of nonlinear equations. In addition, like our second-order boundary approximation, Carmona and Durrleman's method also requires the somewhat expensive calculation of the square root of $\boldsymbol{\Sigma}$. Interpreting $s_{N+1} \equiv K$, the deltas and kappa of the spread option are given by

$$\frac{\partial \Pi}{\partial s_i} = \frac{\mathbf{S}_i}{s_i} \cdot \Phi\left(d^* + (\mathbf{C}^{1/2}\mathbf{z}^*)_i\sigma_i\sqrt{T}\right), \quad i = 0, 1, \ldots, N+1. \tag{52}$$

One very nice feature about this method is that it always gives a lower bound for the actual price. The main difficulty of applying Carmona and Durrleman's method is in solving the system of nonlinear equations, because there is not much guidance on the choice of initial values for d^*, $\mathbf{z}^*$ and μ.

4.2. Numerical performance

We now compare our methods, namely, the extended Kirk approximation and the second-order boundary approximation, with Monte Carlo simulation, numerical integration method based on Proposition 2.1, and Carmona and Durrleman's method. We perform the comparisons for four different dimensions $N+1$, namely, 3, 20, 50, and 150 using an artificial correlation matrix similar to the one used in Carmona and Durrleman (2005). In addition, in order to test various methods using a more plausible correlation matrix, we also apply the methods to two hypothetical spread options. One is between the S&P 500 index and the 30 component stocks of the Dow Jones Industrial Average (DJIA) index and the other is between the S&P SmallCap 600 index and the DJIA components. All methods are implemented in MATLAB 7.0 on a Dell Optiplex GX620 with 3.80 GHz Intel Pentium(R) 4 CPU and 3G RAM. For the purpose of definiteness and the fact that Carmona and Durrleman (2005) only consider the geometric Brownian motions case, we will only compare models in this special case.

Table 1. Prices of spread options on three assets. This table reports the three-asset spread option prices of different methods. Numbers in parenthesis are the relative errors. NI represents two-dimensional numerical integration. EK represents the extended Kirk approximation. SB represents the second-order boundary approximation. CD represents Carmona and Durrleman's method, using the globally convergent Newton–Raphson algorithm to solve the set of nonlinear equations. MC represents Monte Carlo simulation with 10 000 000 replications, whose standard error is in the order of 10^{-3} or 10^{-4}. The time listed is the average computing time of one option price. The asterisk on Carmona and Durrleman's method indicates that the searching time for initial values is not included.

K	$\sigma = 30\%$					$\sigma = 60\%$				
	NI	EK	SB	CD	MC	NI	EK	SB	CD	MC
30	13.5762	13.3426	13.5761	13.5751	13.5767	20.2066	19.6953	20.2063	20.1952	20.2043
		(-2×10^{-2})	(-7×10^{-6})	(-8×10^{-5})	(4×10^{-5})		(-3×10^{-2})	(-1×10^{-5})	(-6×10^{-4})	(-1×10^{-4})
35	10.3573	10.1171	10.3572	10.3560	10.3584	17.4770	16.9978	17.4769	17.4641	17.4759
		(-2×10^{-2})	(-1×10^{-5})	(-1×10^{-4})	(1×10^{-4})		(-3×10^{-2})	(-8×10^{-6})	(-7×10^{-4})	(-6×10^{-5})
40	7.6610	7.4337	7.6610	7.6594	7.6597	15.0280	14.5889	15.0281	15.0135	15.0293
		(-3×10^{-2})	(-1×10^{-6})	(-2×10^{-4})	(-2×10^{-4})		(-3×10^{-2})	(2×10^{-6})	(-1×10^{-3})	(9×10^{-5})
45	5.4914	5.2921	5.4914	5.4897	5.4901	12.8516	12.4580	12.8518	12.8361	12.8514
		(-4×10^{-2})	(-2×10^{-6})	(-3×10^{-4})	(-2×10^{-4})		(-3×10^{-2})	(2×10^{-5})	(-1×10^{-3})	(-2×10^{-5})
50	3.8150	3.6523	3.8150	3.8132	3.8142	10.9347	10.5891	10.9351	10.9186	10.9332
		(-4×10^{-2})	(3×10^{-6})	(-4×10^{-4})	(5×10^{-5})		(-3×10^{-2})	(4×10^{-5})	(-2×10^{-3})	(-1×10^{-4})
Time (s)	21.87	0.00017	0.00034	0.016*	8.06					

Table 2. Greeks of spread options on three assets. This table reports the three-asset spread option Greeks of different methods. Numbers in parenthesis are the relative errors. NI represents two-dimensional numerical integration. EK represents the extended Kirk approximation. SB represents the second-order boundary approximation. CD represents Carmona and Durrleman's method, using the globally convergent Newton–Raphson method to solve the set of nonlinear equations. MC represents Monte Carlo simulation with 10 000 000 replications, whose standard error is around the order of 10^{-4}. The time listed is the average computing time of one Greek. The asterisk on Carmona and Durrleman's method indicates that the searching time for initial values is not included.

Greeks	$\sigma = 30\%$					$\sigma = 60\%$				
	NI	EK	SB	CD	MC	NI	EK	SB	CD	MC
Δ_1	0.7405	0.7436 (4×10^{-3})	0.7404 (-7×10^{-5})	0.7413 (1×10^{-3})	0.7405 (4×10^{-5})	0.6674	0.6619 (-8×10^{-3})	0.6672 (-3×10^{-4})	0.6675 (2×10^{-4})	0.6675 (2×10^{-4})
Δ_2	-0.6786	-0.7025 (4×10^{-2})	-0.6785 (-9×10^{-5})	-0.6776 (-1×10^{-3})	-0.6784 (-2×10^{-4})	-0.5283	-0.5684 (8×10^{-2})	-0.5280 (-5×10^{-4})	-0.5283 (-8×10^{-5})	-0.5284 (2×10^{-4})
Δ_3	-0.7194	-0.7025 (-2×10^{-2})	-0.7193 (-7×10^{-5})	-0.7185 (-1×10^{-3})	-0.7192 (-2×10^{-4})	-0.6195	-0.5684 (-8×10^{-2})	-0.6193 (-4×10^{-4})	-0.6198 (4×10^{-4})	-0.6195 (5×10^{-5})
κ	-0.6938	-0.7058 (2×10^{-2})	-0.6937 (-6×10^{-5})	-0.6929 (-1×10^{-3})	-0.6938 (2×10^{-5})	-0.5741	-0.5759 (3×10^{-3})	-0.5741 (-9×10^{-5})	-0.5745 (5×10^{-4})	-0.5745 (7×10^{-4})
Time (s)	7.62	0.00011	0.00013	0.029*	12.60					

For the Monte Carlo simulation, we generate 10 000 000 replicates. We use Proposition 2.1 rather than equation (10) because if one uses equation (10), then the information on the random variables x and $\mathbf{y}$ is completely lost if the option happens to be out of money. The use of Proposition 2.1 amounts to an importance sampling technique. In the actual implementation we find that it gives very large variance reduction in Π. The numerical integration method is only used for the three-dimensional case because the computational cost is exceedingly high when the dimension is high. The numerical integration results computed with error tolerance level 10^{-8} are used as actual option prices to calculate the relative pricing errors ($\Pi_{\text{Approximation}} - \Pi_{\text{Actual}})/\Pi_{\text{Actual}}$. For Carmona and Durrleman's method, we use the globally convergent Newton–Raphson method as described in Press *et al.* (1992). We find that the globally convergent Newton–Raphson method is slightly more stable than the Newton–Raphson method and slightly faster to converge to the optimal solution. However, the optimization is still extremely sensitive to the choice of initial values and very often fails. The region of initial values that will lead to solutions is an unknown function of the parameters of the spread option, namely, μ_i, ν_i and $\mathbf{\Sigma}$, and unfortunately Carmona and Durrleman (2005) do not give much guidance on how to choose the initial values. Because of this, extensive numerical experiments are often needed to find out the appropriate initial values for different options, which can take from one minute to as long as half an hour. We thus conclude that some guidance on how to choose the initial values in Carmona and Durrleman's method is crucial for the method to be useful in large scale real-life computations.

4.2.1. Spread options on three assets.

As a first example, we consider spread options on three assets. We set $T = 0.25$, $r = 5\%$, and the dividend rates zero. The initial asset prices are $s_0 = 150$, $s_1 = 60$, and $s_2 = 50$. The volatilities of all three assets are given by the same σ and we vary σ to be 0.3 and 0.5. We vary K to be from 30 to 50 with increment 5. The correlation matrix for the asset returns is given by

$$\mathbf{\Sigma} = \begin{pmatrix} 1 & 0.2 & 0.8 \\ 0.2 & 1 & 0.4 \\ 0.8 & 0.4 & 1 \end{pmatrix}.$$

Table 1 reports the prices for each of the five methods we compare together with the average computing times.
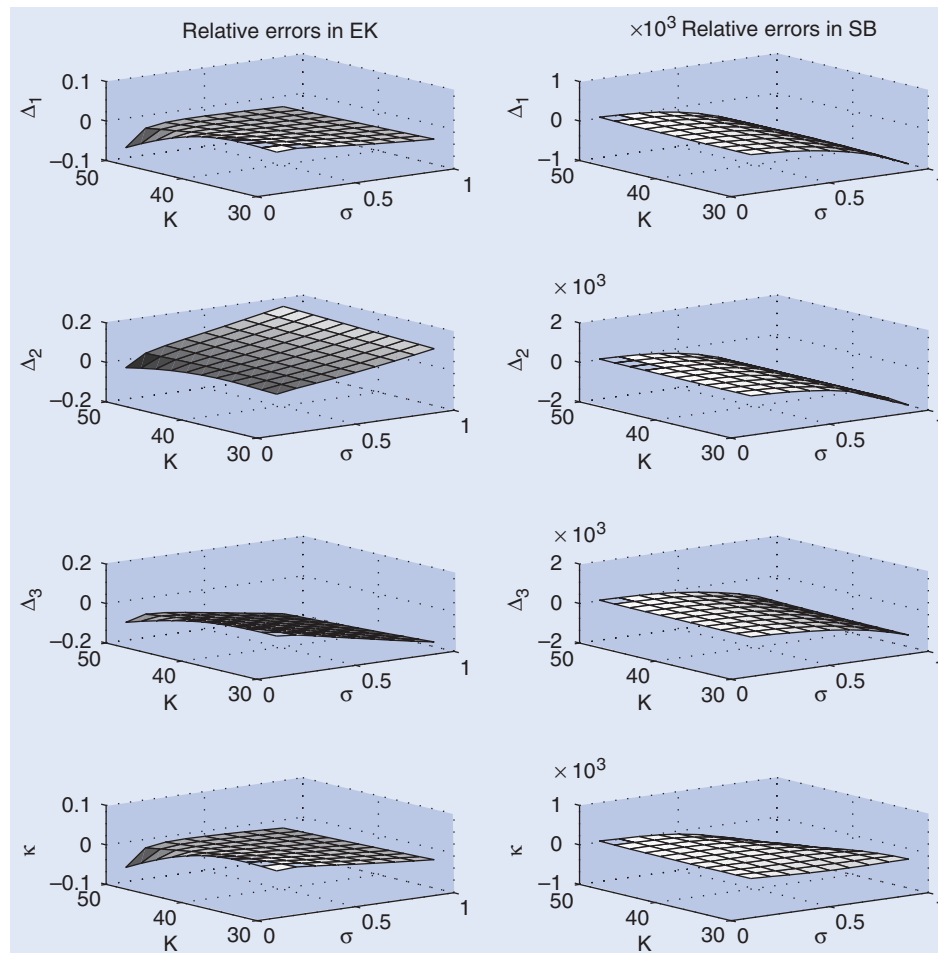

Figure 2. Accuracy comparison of deltas and kappa between the extended Kirk (EK) approximation and the second-order boundary (SB) approximation. The actual values for the Greeks are computed using numerical integration.

The numerical integration results are used as the actual prices. Looking at the relative errors, both our methods are quite accurate with the second-order boundary approximation being more accurate than the extended Kirk approximation. In particular, the relative pricing error of the extended Kirk approximation is in the order of 10^{-2}, while that of the second-order boundary approximation is in the order of 10^{-5}. Monte Carlo simulation with 10 000 000 replications and the use of Proposition 2.1 gives quite accurate results, but usually still not as accurate as the second-order boundary approximation. Carmona and Durrleman's method is also quite accurate but not as good as our second-order boundary approximation. Furthermore, in the actual implementation we need to spend about 20 min to find good starting values for the nonlinear equations that

one has to solve in their method. Even if good starting values are found, their method is still slower than both our methods. The average computing times for both our methods are in the order of 10^{-3} s, while both the numerical integration and Monte Carlo simulation methods take considerably more time.

Table 2 lists the results for four important Greeks for all the methods, namely, the three deltas and the kappa. Here we fix $K = 30$. Again, the qualitative conclusions are the same for the prices. Both our methods are extremely fast, with the second-order boundary approximation giving the most accurate results. Figure 2 further compares the accuracy of the four important Greeks between the extended Kirk approximation and the second-order boundary approximation. Parameters are still the same, but now K varies in the range [30, 50] and

Table 3. Prices of spread options on 20, 50 and 150 assets. This table reports the spread option prices of different methods when the numbers of assets are 20, 50 and 150. EK represents the extended Kirk approximation. SB represents the second-order boundary approximation. CD represents Carmona and Durrleman's method, using the globally convergent Newton–Raphson method to solve the set of nonlinear equations. MC represents Monte Carlo simulation with 10 000 000 replications. Numbers in parenthesis are the standard errors for MC. The time listed is the average computing time of one option price. The asterisk on Carmona and Durrleman's method indicates that the searching time for initial values is not included.

K	$\sigma = 30\%$				$\sigma = 60\%$			
	EK	SB	CD	MC	EK	SB	CD	MC
Panel A: 20 assets								
0	15.1119	15.1132	15.1122	15.1131 (2×10^{-4})	23.9279	23.9394	23.9283	23.9398 (1×10^{-3})
5	12.1229	12.1243	12.1233	12.1242 (2×10^{-4})	21.3570	21.3684	21.3577	21.3683 (1×10^{-3})
10	9.5495	9.5509	9.5498	9.5512 (2×10^{-4})	19.0032	19.0144	19.0038	19.0144 (1×10^{-3})
15	7.3867	7.3881	7.3870	7.3882 (2×10^{-4})	16.8596	16.8706	16.8603	16.8712 (1×10^{-3})
20	5.6119	5.6132	5.6122	5.6132 (2×10^{-4})	14.9173	14.9280	14.9180	14.9279 (1×10^{-3})
Time (s)	0.00018	0.00069	0.57*	51.81				
Panel B: 50 assets								
0	28.5062	28.5078	28.5070	28.5077 (6×10^{-4})	51.4195	51.4316	51.4211	51.4309 (3×10^{-3})
5	25.8944	25.8959	25.8952	25.8950 (6×10^{-4})	49.0466	49.0586	49.0482	49.0621 (3×10^{-3})
10	23.4514	23.4529	23.4522	23.4529 (6×10^{-4})	46.7603	46.7722	46.7620	46.7748 (3×10^{-3})
15	21.1754	21.1769	21.1761	21.1774 (6×10^{-4})	44.5593	44.5712	44.5611	44.5731 (3×10^{-3})
20	19.0633	19.0647	19.0641	19.0652 (6×10^{-4})	42.4423	42.4541	42.4442	42.4522 (3×10^{-3})
Time (s)	0.00021	0.0032	7.39*	136.24				
Panel C: 150 assets								
0	74.6046	74.6062	74.6066	74.6044 (2×10^{-3})	143.8020	143.8143	143.8070	143.8064 (8×10^{-3})
5	72.1642	72.1657	72.1666	72.1688 (2×10^{-3})	141.5173	141.5296	141.5239	141.5421 (8×10^{-3})
10	69.7800	69.7815	69.7818	69.7818 (2×10^{-3})	139.2615	139.2737	139.2653	139.2741 (8×10^{-3})
15	67.4519	67.4534	67.4544	67.4537 (2×10^{-3})	137.0342	137.0464	137.0404	137.0471 (8×10^{-3})
20	65.1795	65.1810	65.1820	65.1811 (2×10^{-3})	134.8354	134.8477	134.8396	134.8473 (8×10^{-3})
Time (s)	0.00038	0.035	292.91*	452.10				

σ varies in the range $[0.1, 0.9]$. The actual values for the Greeks are computed using numerical integration. The Greeks for the extended Kirk approximation are obtained by differentiating equation (18) in Proposition 3.1. The Greeks for the second-order boundary approximation are given in Proposition 3.5. The Greeks for Carmona and Durrleman's method are given in equation (52). Figure 2 indicates that for the purpose of calculating the Greeks, the second-order boundary approximation should be preferred to the extended Kirk approximation.

4.2.2. Spread options on 20, 50 and 150 assets. Next, we consider spread options on multiple assets with numbers of assets $N+1$ equal 20, 50 and 150, respectively. We will consider symmetric target assets with initial prices $s_0 = 10(N+1)$ and $s_1 = \cdots = s_N = 10$. We set $T = 0.25$, $r = 5\%$, and dividend rates zero. The correlation matrix is set to be

$$\Sigma = \begin{pmatrix} 1 & \rho & \cdots & \rho \\ \rho & 1 & \ddots & \vdots \\ \vdots & \vdots & \ddots & \rho \\ \rho & \cdots & \rho & 1 \end{pmatrix} \qquad (53)$$

with $\rho = 0.4$. All assets returns have the same volatility σ and we vary σ to be either 0.3 or 0.6. We vary K from 0 to 20 with increment 5.

Table 3 reports the prices of spread options with different numbers of assets, different volatilities σ and strikes K for each of the four methods we consider, together with the average computing time of each method. The results for different dimension $N+1$ are reported in three different panels. Since N is large,

numerical integration is no longer feasible so we do not know the exact actual option prices and as a result, we do not know the exact relative pricing errors. However, the results from Monte Carlo simulation can serve as a rough comparison benchmark. The results indicate that when the target assets are more symmetric, the extended Kirk approximation is more accurate. Again, both our methods are among the fastest and the second-order boundary approximation is much more accurate than the extended Kirk approximation and Carmona and Durrleman's method.
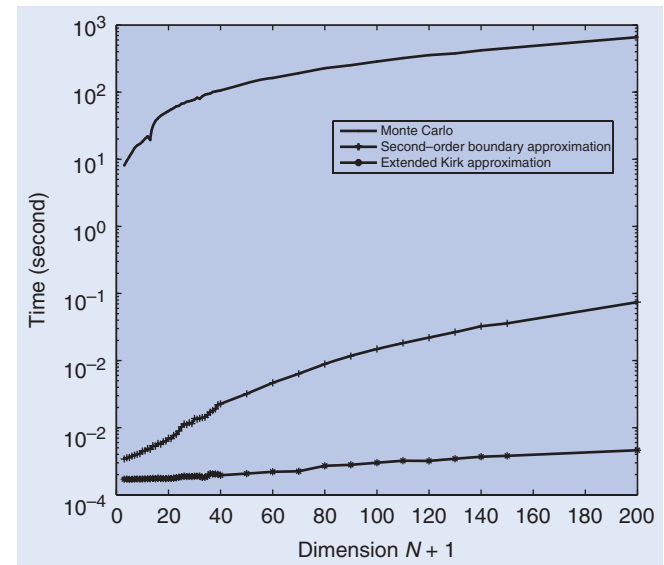

Figure 3. Average computing time as a function of dimension $N+1$ for one spread option in Monte Carlo simulation, the extended Kirk approximation and the second-order boundary approximation.

Table 4. Prices of spread options on S&P 500 and DJIA components. This table reports the spread option prices of different methods, where the options are written between the S&P 500 index and the Dow Jones Industrial Average (DJIA) component stocks. EK represents the extended Kirk approximation. SB represents the second-order boundary approximation. CD represents Carmona and Durrleman's method, using the globally convergent Newton–Raphson method to solve the set of nonlinear equations. MC represents Monte Carlo simulation with 10 000 000 replications. Numbers in parenthesis are the standard errors for MC. The time listed is the average computing time of one option price. The asterisk on Carmona and Durrleman's method indicates that the searching time for initial values is not included.

K	$T = 1/6$				$T = 1/3$			
	EK	SB	CD	MC	EK	SB	CD	MC
0	49.7453	50.1471	50.1336	50.1464 (6×10^{-3})	53.5266	53.5267	53.4684	53.5260 (8×10^{-3})
15	36.5853	37.2481	37.2276	37.2481 (5×10^{-3})	40.7162	41.9215	41.8499	41.9211 (7×10^{-3})
30	24.9909	25.9129	24.8859	25.9125 (5×10^{-3})	30.2193	31.6552	31.5736	31.6558 (6×10^{-3})
45	15.5874	16.6634	16.6329	16.6635 (4×10^{-3})	21.3773	22.9449	22.8581	22.9449 (5×10^{-3})
60	8.7325	9.7825	9.7531	9.7820 (3×10^{-3})	14.3348	15.9007	15.8156	15.9045 (4×10^{-3})
75	4.3312	5.1864	5.1628	5.1866 (2×10^{-3})	9.0686	10.4988	10.4218	10.5013 (3×10^{-3})
90	1.8802	2.4619	2.4457	2.4622 (1×10^{-3})	5.3921	6.5866	6.5227	6.5874 (2×10^{-3})
Time (s)	0.00019	0.0013	1.71*	82.83				

Table 5. Prices of spread options on S&P SmallCap 600 and DIJA components. This table reports the spread option prices of different methods, where the options are written between the S&P SmallCap 600 index and the Dow Jones Industrial Average (DJIA) component stocks. EK represents the extended Kirk approximation. SB represents the second-order boundary approximation. CD represents Carmona and Durrleman's method, using the globally convergent Newton–Raphson method to solve the set of nonlinear equations. MC represents Monte Carlo simulation with 10 000 000 replications. Numbers in parenthesis are the standard errors for MC. The time listed is the average computing time of one option price. The asterisk on Carmona and Durrleman's method indicates that the searching time for initial values is not included.

	$T=1/6$				$T=1/3$			
K	EK	SB	CD	MC	EK	SB	CD	MC
0	46.7497	47.0864	47.0697	47.0878 (8×10^{-3})	61.0999	61.6068	61.5581	61.6163 (1×10^{-2})
30	31.1304	31.4923	31.4754	31.4994 (7×10^{-3})	45.8508	46.3877	46.3389	46.3960 (9×10^{-3})
60	19.4500	19.7945	19.7799	19.7963 (5×10^{-3})	33.3758	33.9092	33.8627	33.9161 (8×10^{-3})
90	11.3518	11.6436	11.6315	11.6475 (3×10^{-3})	23.5374	24.0361	23.9946	24.0426 (6×10^{-3})
120	6.1692	6.3901	6.3811	6.3914 (6×10^{-3})	16.0680	16.5082	16.4726	16.5094 (4×10^{-3})
150	3.1157	3.2657	3.2599	3.2668 (1×10^{-3})	10.6130	10.9806	10.9517	10.9851 (3×10^{-3})
180	1.4610	1.5529	1.5494	1.5535 (7×10^{-4})	6.7817	7.0730	7.0511	7.0735 (2×10^{-3})
Time (s)	0.00019	0.0013	1.71*	82.83				

Figure 3 gives the computing time as a function of dimension $N+1$. The dimension $N+1$ varies from 3 to 200. The vertical axis is time in log scale. We do not plot the computing times for Carmona and Durrleman's method because it often takes more than 20 min to search for good initial starting values for their algorithm. If we do not include the search time, which is significant, the curve for Carmona and Durrleman's method would lie somewhere between the second-order boundary approximation and Monte Carlo simulation. As we see, up to dimension 25, both our methods take less than 10^{-3} s to compute the price of one spread option. The extended Kirk approximation remains within 10^{-3} s for all dimensions, while the second-order boundary approximation remains within 10^{-1} s. Monte Carlo simulation takes considerably more time, ranging from 8 s in dimension 3 to over 500 s in dimension 200. For all dimensions, the computing times in the extended Kirk approximation are about 0.001% or 0.0001% of those in Monte Carlo simulation while the computing times in the second-order boundary approximation are about 0.01% of those in Monte Carlo simulation.

4.2.3. Spread options on two S&P indices and DJIA components. Our final numerical example considers two hypothetical spread options. The first one is written on the S&P 500 index and the 30 component stocks of the Dow Jones Industrial Average (DJIA) index. The second one is written on the S&P SmallCap 600 index and DJIA components. Both options are very interesting in practice because industrial practitioners pay very close and constant attention to the different performances among large company stocks, small company stocks and the whole market. For our numerical experiments, these options are very interesting because now the target assets are not completely symmetric.

For the first spread options, the final payoff is given by $[S_0(T) - \sum_{k=1}^{30} S_k(T) - K]^+$, where S_0 is chosen to be the S&P 500 index multiplied by 1.15, and $S_1, \ldots, S_{30}$ the prices of the DJIA component stocks. The weight 1.15 is chosen such that the spread option is near the money. Because of occasional additions and deletions of the DJIA components, the DJIA component stocks are fixed as those on August 29, 2007. For the second spread option, S_0 is chosen to be the S&P SmallCap 600 index multiplied by 4.

We consider two different maturities, $T=1/6$ and $T=1/3$. For each maturity T, to obtain μ_k and ν_k, we use equation (2) and compute the mean and variance of the historical T-period returns $R_{k,T}$. For the first option, we use historical daily price data from the CRSP (Center for Research in Security Prices) data base from July 9, 1986 to August 29, 2007 because the stock prices for several companies are only available after July 9, 1986. The returns are calculated using daily close prices after adjusting for stock splits. The prices on August 29, 2007 are used to determine the initial asset prices s_k's. Alternatively, we could have used equations (5) to compute μ_k's and ν_k's by estimating the dividend rates. The correlation matrix Σ is estimated from the historical correlation matrix of the $R_{k,T}$'s. For the second option, we use historical daily price data from August 16, 1995 to August 29, 2007 because the S&P SmallCap 600 index is only available after August 16, 1995. To include both in-the-money and out-of-the-money options, we vary K from 0 to 75 with increment 15 for the first option, and vary K from 0 to 120 with increment 30 for the second one.

Tables 4 and 5 report the prices of the two spread option with different maturities T and strikes K, together

with the average computing time of each method. Because actual prices are not available, we use the results from the Monte Carlo simulation as a rough benchmark. As we see, the extended Kirk approximation in this nonsymmetric case becomes less accurate, with relative pricing error sometimes quite significant. Our second-order boundary approximation generally gives a more accurate approximation for the option prices than Carmona and Durrleman's method.

5. Conclusion

In this paper, we study spread options written on multiple assets. We develop two closed-form approximations for pricing them, namely, the extended Kirk approximation and the second-order boundary approximation. The latter approximation generalizes the results in Li *et al.* (2008) to spread options on arbitrary number of assets. Numerical analysis demonstrates that both of our methods are very robust, fast and accurate, with the second-order approximation being more accurate than the extended Kirk approximation and other existing methods. For spread options written on three assets, the relative pricing error of the second-order approximation is in the order of 10^{-4} with an average computing time for each option of 2×10^{-4} s. For dimensions up to about 100, the second-order boundary approximation takes less than 10^{-2} s. Thus, our method enables the accurate pricing of a bulk volume of spread options on multiple assets with different contract specifications in real time, which offers traders a potential edge in financial markets. We also extend our results to hybrid spread-basket options.

In addition, our approximations, especially the second-order boundary approximation, can be used to approximate the Greeks of spread options, which serve as valuable tools in financial applications such as calculating the delta-hedging position of a portfolio containing spread options.

There are a few directions that one can take to extend and improve the results in this paper. First, in the geometric Brownian motion case, our results can be easily extended to incorporate jumps in the price processes of the assets. Second, the boundary approximation idea might be useful for pricing other types of more exotic derivatives. Third, it is interesting to consider the effect of nonnormality on a multi-asset spread option. One way to do this is through the multi-variate Gram-Charlier approximation introduced in Li (2008). We leave these to future research.

Acknowledgements

References

Black, F. and Scholes, M., The pricing of options and corporate liabilities. *J. Polit. Econ*, 1973, **81**, 637–659.

Carmona, R. and Durrleman, V., Pricing and hedging spread options. *SIAM Rev.*, 2003, **45**, 627–685.

Carmona, R. and Durrleman, V., Generalizing the Black–Scholes formula to multivariate contigent claims. *J. Comput. Finan.*, 2005, **9**, 42–63.

Deng, S.J., Johnson, B. and Sogomonian, A., Exotic electricity options and the valuation of electricity generation and transmission assets. *Decision Support Syst.*, 2001, **30**, 383–392.

Girma, P.B. and Paulson, A.S., Risk arbitrage opportunities in petroleum futures spreads. *J. Futures Mark.*, 1999, **18**, 931–955.

Greene, W.H., *Econometric Analysis*, 2000 (Prentice Hall: New Jersey).

Jarrow, R. and Rudd, A., Approximate option valuation for arbitrary stochastic processes. *J. Financ. Econ.*, 1982, **10**, 347–369.

Johnson, S.A. and Tian, Y.S., Indexed executive stock options. *J. Financ. Econ.*, 2000, **57**, 35–64.

Johnson, R.L., Zulauf, C.R., Irwin, S.H. and Gerlow, M.E., The soy-bean complex spread: an examination of market efficiency from the viewpoint of a production process. *J. Futures Mark.*, 1991, **11**, 25–37.

Kirk, E., Correlations in the energy markets, *Managing Energy Price Risk*, pp. 71–78, 1995 (Risk Publications and Enron: London).

Li, M., The impact of return nonnormality on exchange options. *J. Futures Mark.*, 2008, **28**, 845–870.

Li, M., Deng, S.J. and Zhou, J., Closed-form approximations for spread option prices and Greeks. *J. Deriv.*, 2008, **15**, 58–80.

Margrabe, W., The value of an option to exchange one asset for another. *J. Finan.*, 1978, **33**, 177–186.

Mbafeno, A., Co-movement term structure and the valuation of energy spread options, In *Mathematics of Derivative Securities*, edited by M. Dempster and S. Pliska, 1997 (University Press: Cambridge, UK).

Pearson, N., An efficient approach for pricing spread options. *J. Deriv.*, 1995, **3**, 76–91.

Press, W.H., Flannery, B.P., Teukolsky, S.A. and Vetterling, W.T., Numerical Recipes in C: The Art of Scientific Computing, 1992.

Routledge, S., Seppi, D.J. and Spatt, C.S., The 'Spark Spread': an equilibrium model of cross-commodity price relationship in electricity. *Working Paper*, 2001.

Shimko, D., Options on futures spreads: hedging, speculation, and valuation. *J. Futures Mark.*, 1994, **14**, 183–213.

Wilcox, D., *Energy Futures and Options: Spread Options in Energy Markets*, 1990 (Goldman Sachs & Co.: New York).

Zhang, P.G., *Exotic Options: A Guide to Second Generation Options*, pp. 489–499, 1997 (World Scientific: Singapore).

Appendix A: Proofs

Proof of Proposition 2.1: The conditional density of X given $Y = \mathbf{y}$ is $\phi(x; \mu_{x|\mathbf{y}}, \Sigma_{x|\mathbf{y}})$, i.e. a normal density with mean $\mu_{x|\mathbf{y}}$ and variance $\Sigma_{x|\mathbf{y}}$. By formula for the determinants for partitioned matrix, we have $\Sigma_{x|\mathbf{y}} \neq 0$ since

$$\det \Sigma = \det(\Sigma_{11} - \Sigma_{10}\Sigma_{10}') = (\det(\Sigma_{11}))^{-1}\Sigma_{x|\mathbf{y}} \neq 0.$$

Thus, we can compute the price of the spread option as follows:

$$\Pi = e^{-rT}\int_{\mathbb{R}^N}\int_{\mathbb{R}}\left(e^{v_0 x + \mu_0} - \sum_{k=1}^{N}e^{v_k y_k + \mu_k} - K\right)^{+}$$
$$\times \phi(\{x, \mathbf{y}\}; \mathbf{0}, \Sigma)\mathrm{d}x\,\mathrm{d}\mathbf{y}$$
$$= e^{-rT}\int_{\mathbb{R}^N}\phi(\mathbf{y}; \mathbf{0}, \Sigma_{11})\mathrm{d}\mathbf{y}\int_{\underline{x}(\mathbf{y})}^{\infty}\left(e^{v_0 x + \mu_0} - \sum_{k=1}^{N}e^{v_k y_k + \mu_k} - K\right)$$
$$\times \phi(x; \mu_{x|\mathbf{y}}, \Sigma_{x|\mathbf{y}})\mathrm{d}x.$$

By virtue of the identity

$$\int_{x_0}^{\infty}e^{tx}n(x; \mu, \sigma^2)\mathrm{d}x = e^{\mu t + \sigma^2 t^2/2}\Phi\left(\frac{\mu - x_0}{\sigma} + \sigma t\right), \quad \text{(A1)}$$

the inner integral can be performed to yield

$$\Pi = e^{(1/2v_0^2\Sigma_{x|y}) + \mu_0 - rT}\int_{\mathbb{R}^N}e^{v_0\mu_{x|y}}$$
$$\times \phi(\mathbf{y}; \mathbf{0}, \Sigma_{11})\,\Phi\left(A(\mathbf{y}) + v_0\sqrt{\Sigma_{x|y}}\right)\mathrm{d}\mathbf{y}$$
$$- \sum_{k=1}^{N}e^{-rT}\int_{\mathbb{R}^N}e^{v_k y_k + \mu_k}\,\phi(\mathbf{y}; \mathbf{0}, \Sigma_{11})\,\Phi\left(A(\mathbf{y})\right)\mathrm{d}\mathbf{y}$$
$$- Ke^{-rT}\int_{\mathbb{R}^N}\phi(\mathbf{y}; \mathbf{0}, \Sigma_{11})\,\Phi\left(A(\mathbf{y})\right)\mathrm{d}\mathbf{y}. \quad \text{(A2)}$$

Completing the square after a change of variable $\mathbf{z} = \mathbf{y} - v_0\Sigma_{10}$ gives

$$e^{(1/2v_0^2\Sigma_{x|y}) + \mu_0 - rT}\int_{\mathbb{R}^N}e^{v_0\mu_{x|y}}\,\phi(\mathbf{y}; \mathbf{0}, \Sigma_{11})\,\Phi\left(A(\mathbf{y}) + v_0\sqrt{\Sigma_{x|y}}\right)\mathrm{d}\mathbf{y}$$
$$= e^{-rT + \mu_0 + \frac{1}{2}v_0^2}\int_{\mathbb{R}^N}\phi(\mathbf{z}; \mathbf{0}, \Sigma_{11})\Phi\left(A(\mathbf{z} + v_0\Sigma_{10}) + v_0\sqrt{\Sigma_{x|y}}\right)\mathrm{d}\mathbf{z}.$$

Similarly, a change of variable $\mathbf{z} = \mathbf{y} - v_k\Sigma_{11}\mathbf{e}_k$, for $k = 1, 2, \ldots, N$, gives

$$e^{-rT}\int_{\mathbb{R}^N}e^{v_k y_k + \mu_k}\,\phi(\mathbf{y}; \mathbf{0}, \Sigma_{11})\,\Phi\left(A(\mathbf{y})\right)\mathrm{d}\mathbf{y}$$
$$= e^{-rT + \mu_k + \frac{1}{2}v_k^2}\int_{\mathbb{R}^N}\phi(\mathbf{z}; \mathbf{0}, \Sigma_{11})\Phi\left(A(\mathbf{z} + v_k\Sigma_{11}\mathbf{e}_k)\right)\mathrm{d}\mathbf{z}.$$

Collecting terms, we get the expressions in Proposition 2.1.

Proof of Proposition 3.1: Consider a spread option on two assets with final payoff $(S_0(T) - L(T) - K)^{+}$, where $\log S_0(T)$ and $\log L(T)$ are jointly normal with means μ_0, μ_a, variances v_0^2, v_a^2, and correlation ρ_a. Then the two-asset Kirk approximation for the spread option price is given by

$$e^{\mu_0 + \frac{1}{2}v_0^2 - rT}\Phi(d_1) - (e^{\mu_a + \frac{1}{2}v_a^2 - rT} + Ke^{-rT})\Phi(d_2),$$

where

$$d_1 = \frac{1}{v_K}\log\left(\frac{e^{\mu_0 + \frac{1}{2}v_0^2 - rT}}{e^{\mu_a + \frac{1}{2}v_a^2 - rT} + Ke^{-rT}}\right) + \frac{1}{2}v_K, \quad d_2 = d_1 - v_K,$$

with

$$v_K = \sqrt{v_0^2 + m^2 v_a^2 - 2m\rho_a v_0 v_a} \quad \text{and} \quad m = \frac{e^{\mu_a + \frac{1}{2}v_a^2 - rT}}{e^{\mu_a + \frac{1}{2}v_a^2 - rT} + Ke^{-rT}}.$$

To apply the above result for multi-asset spread options with payoff $(S_0(T) - \sum_{k=1}^{N}S_N(T) - K)^{+}$, we let $L(T) = \sum_{k=1}^{N}S_k(T)$. A common technique is to approximate the arithmetic average $\sum_{k=1}^{N}S_k(T)/N$ by the geometric average $\prod_{k=1}^{N}S_k(T)^{1/N}$.

For v_a, notice that

$$v_a^2 = \mathrm{Var}(\log L(T)) \approx \mathrm{Var}\left(\log\left(N\prod_{k=1}^{N}S_k(T)^{1/N}\right)\right)$$
$$= \mathrm{Var}\left(\frac{1}{N}\sum_{k=1}^{N}\log S_k(T)\right) = \frac{1}{N^2}\sum_{i=1}^{N}\sum_{j=1}^{N}\rho_{i,j}v_i v_j.$$

For ρ_a, notice that

$$\rho_a = \frac{1}{v_0 v_a}\mathrm{Cov}(\log S_0(T), \log L(T))$$
$$\approx \frac{1}{v_0 v_a}\mathrm{Cov}\left(\log S_0(T), \log\prod_{k=1}^{N}S_k(T)^{1/N}\right)$$
$$= \frac{1}{v_0 v_a}\mathrm{Cov}\left(\log S_0(T), \frac{1}{N}\sum_{k=1}^{N}\log S_k(T)\right)$$
$$= \frac{1}{Nv_a}\sum_{k=1}^{N}\rho_{0,k}v_k.$$

To compute μ_a, notice that since $\log L(T)$ is approximated normally distributed with mean μ_a and variance v_a^2, we have $\mathbb{E}\,e^{\log L(T)} \approx e^{\mu_a + v_a^2/2}$. Thus,

$$\mu_a \approx \log \mathbb{E}\,e^{\log L(T)} - \frac{1}{2}v_a^2 = \log \mathbb{E}\sum_{k=1}^{N}S_k(T) - \frac{1}{2}v_a^2$$
$$= \log\left(\sum_{k=1}^{N}e^{\mu_k + \frac{v_k^2}{2}}\right) - \frac{1}{2}v_a^2.$$

The final step of the proof involves simplifying the expressions for m and m_0 using the expression for μ_a.

Proof of Proposition 3.2: This proposition follows directly from Taylor expanding the exercise boundary (9) to second order in $\mathbf{y}$ around $\mathbf{y} = \mathbf{0}$:

$$(\nabla \underline{x}|_{\mathbf{0}})_k = \frac{\partial \underline{x}}{\partial y_k}\Big|_{\mathbf{0}} = \frac{e^{\mu_k}v_k}{v_0(R + K)}, \quad k = 1, 2, \ldots, N,$$

$$(\nabla^2 \underline{x}|_{\mathbf{0}})_{i,j} = \frac{\partial^2 \underline{x}}{\partial y_i \partial y_j}\Big|_{\mathbf{0}} = -\frac{v_i v_j e^{\mu_i + \mu_j}}{v_0(R + K)^2} + \delta_{i,j}\frac{v_j^2 e^{\mu_j}}{v_0(R + K)},$$

$$i, j = 1, 2, \ldots, N.$$

Proof of Proposition 3.3: From Proposition 2.1, we have

$$\Pi = e^{-rT+\mu_0+\frac{1}{2}\nu_0^2}\,\mathbf{I}_0 - \sum_{k=1}^N e^{-rT+\mu_k+\frac{1}{2}\nu_k^2}\,\mathbf{I}_k - Ke^{-rT}\,\mathbf{I}_{N+1}.$$

First, by Proposition 3.2, $A(\mathbf{y}) \approx c + \mathbf{d}'\mathbf{y} + \mathbf{y}'\mathbf{E}\mathbf{y}$. Next, we treat $\mathbf{y}'\mathbf{E}\mathbf{y}$ as an independent quantity from $c + \mathbf{d}'\mathbf{y}$ and expand $\Phi(A(\mathbf{y})) \approx \Phi(c + \mathbf{d}'\mathbf{y} + \mathbf{y}'\mathbf{E}\mathbf{y})$ to second order in $\mathbf{y}'\mathbf{E}\mathbf{y}$ around

$$\mathbf{y}'\mathbf{E}\mathbf{y} = \epsilon = \int_{\mathbb{R}^N} \phi(\mathbf{y};\mathbf{0},\mathbf{\Sigma}_{11})\mathbf{y}'\mathbf{E}\mathbf{y}\,d\mathbf{y} = tr(\mathbf{F}).$$

Since

$$\left.\frac{d\Phi(c+\mathbf{d}'\mathbf{y}+\mathbf{y}'\mathbf{E}\mathbf{y})}{d\mathbf{y}'\mathbf{E}\mathbf{y}}\right|_{\mathbf{y}'\mathbf{E}\mathbf{y}=\epsilon} = \phi(c+\epsilon+\mathbf{d}'\mathbf{y}),$$

$$\left.\frac{d^2\Phi(c+\mathbf{d}'\mathbf{y}+\mathbf{y}'\mathbf{E}\mathbf{y})}{d(\mathbf{y}'\mathbf{E}\mathbf{y})^2}\right|_{\mathbf{y}'\mathbf{E}\mathbf{y}=\epsilon} = -(c+\epsilon+\mathbf{d}'\mathbf{y})\,\phi(c+\epsilon+\mathbf{d}'\mathbf{y}),$$

we have

$$\mathbf{I}_{N+1} = \int_{\mathbb{R}^N} \phi(\mathbf{y};\mathbf{0},\mathbf{\Sigma}_{11})\Phi(A(\mathbf{y}))d\mathbf{y} \tag{A3}$$

$$\approx \int_{\mathbb{R}^N} \phi(\mathbf{y};\mathbf{0},\mathbf{\Sigma}_{11})\Phi(c+\mathbf{d}'\mathbf{y}+\mathbf{y}'\mathbf{E}\mathbf{y})d\mathbf{y} \tag{A4}$$

$$\approx \int_{\mathbb{R}^N} \phi(\mathbf{y};\mathbf{0},\mathbf{\Sigma}_{11})\Big[\Phi(c+\epsilon+\mathbf{d}'\mathbf{y}) + \phi(c+\epsilon+\mathbf{d}'\mathbf{y})$$

$$(\mathbf{y}'\mathbf{E}\mathbf{y}-\epsilon) - \frac{1}{2}(c+\epsilon+\mathbf{d}'\mathbf{y})$$

$$\phi(c+\epsilon+\mathbf{d}'\mathbf{y})(\mathbf{y}'\mathbf{E}\mathbf{y}-\epsilon)^2\Big]d\mathbf{y} \tag{A5}$$

$$\equiv \mathbf{J}_{N+1}^0 + \mathbf{J}_{N+1}^1 - \frac{1}{2}\mathbf{J}_{N+1}^2, \tag{A6}$$

where

$$\mathbf{J}_{N+1}^0 = \int_{\mathbb{R}^N} \phi(\mathbf{y};\mathbf{0},\mathbf{\Sigma}_{11})\Phi(c+\epsilon+\mathbf{d}'\mathbf{y})d\mathbf{y},$$

$$\mathbf{J}_{N+1}^1 = \int_{\mathbb{R}^N} \phi(\mathbf{y};\mathbf{0},\mathbf{\Sigma}_{11})\,\phi(c+\epsilon+\mathbf{d}'\mathbf{y})\,(\mathbf{y}'\mathbf{E}\mathbf{y}-\epsilon)d\mathbf{y},$$

$$\mathbf{J}_{N+1}^2 = \int_{\mathbb{R}^N} \phi(\mathbf{y};\mathbf{0},\mathbf{\Sigma}_{11})(c+\epsilon+\mathbf{d}'\mathbf{y})\,\phi(c+\epsilon+\mathbf{d}'\mathbf{y})(\mathbf{y}'\mathbf{E}\mathbf{y}-\epsilon)^2d\mathbf{y}.$$

Notice that in going from equation (A3) to equation (A4), we have used the second-order boundary approximation in Proposition 3.2. Strictly speaking, another approximation (a Taylor series approximation) is used in going from equation (A4) to equation (A5).

Before we compute the $\mathbf{J}^i$'s, we give some important remarks on our approximation. Notice that the above derivation reveals that our approximation is convergent in the sense that if we keep more and more higher-order terms, then the resulting approximating prices will approach the true value of $\mathbf{I}_{N+1}$, provided that parameters are within the convergence radii. In particular, we would need that the nonlinearity of $A(\mathbf{y})$ is relatively mild.

We now turn to the computation of the $\mathbf{J}^i$'s. For $\mathbf{J}_{N+1}^0$, a change of variable $w = \mathbf{d}'\mathbf{y}$ gives

$$\mathbf{J}_{N+1}^0 = \int_{\mathbb{R}} \phi(w;0,\mathbf{d}'\mathbf{\Sigma}_{11}\mathbf{d})\Phi(c+\epsilon+w)dw. \tag{A7}$$

The following result in Li (2008) is very useful and we refer readers to Li (2008) for a proof:

$$\int_{-\infty}^\infty \Phi(a+by)\phi(y;\mu,\sigma^2)\,dy = \Phi\left(\frac{a+b\mu}{\sqrt{1+b^2\sigma^2}}\right).$$

With the help of the above identity, the integral in (A7) can be performed to give

$$\mathbf{J}_{N+1}^0 = \Phi\left(\frac{c+\epsilon}{\sqrt{1+\mathbf{d}'\mathbf{\Sigma}_{11}\mathbf{d}}}\right) = \Phi\left(\frac{c_{N+1}}{\sqrt{1+\mathbf{d}_{N+1}'\mathbf{d}_{N+1}}}\right)$$

$$= \mathbf{J}^0(c_{N+1},\mathbf{d}_{N+1}). \tag{A8}$$

For $\mathbf{J}_{N+1}^1$, a change of variable $\mathbf{z} = \mathbf{\Sigma}_{11}^{-1/2}\mathbf{y}$ gives

$$\mathbf{J}_{N+1}^1 = \int_{\mathbb{R}^N} \phi(\mathbf{z};\mathbf{0},\mathbf{I})\,\phi(c+\epsilon+\mathbf{d}_{N+1}'\mathbf{z})\,(\mathbf{z}'\mathbf{F}\mathbf{z}-\epsilon)d\mathbf{z} \tag{A9}$$

$$= \int_{\mathbb{R}^N} \phi(\mathbf{z};\mathbf{0},\mathbf{I})\,\phi(c+\epsilon+\mathbf{d}_{N+1}'\mathbf{z})\,(\mathbf{z}'\mathbf{F}\mathbf{z})d\mathbf{z}$$

$$- \frac{\epsilon}{\sqrt{1+\mathbf{d}_{N+1}'\mathbf{d}_{N+1}}}\,\phi\left(\frac{c_{N+1}}{\sqrt{1+\mathbf{d}_{N+1}'\mathbf{d}_{N+1}}}\right). \tag{A10}$$

We now perform a second change of variable $\mathbf{z} = \mathbf{a} + \mathbf{P}\mathbf{w}$, where

$$\mathbf{P} = (\mathbf{I} + \mathbf{d}_{N+1}\mathbf{d}_{N+1}')^{-1/2}, \quad \mathbf{a} = -(c+\epsilon)\mathbf{P}^2\mathbf{d}_{N+1}.$$

This choice of $\mathbf{P}$ and $\mathbf{a}$ gives

$$(c+\epsilon+\mathbf{d}_{N+1}'\mathbf{z})^2 + |\mathbf{z}|^2 = |\mathbf{w}|^2.$$

The determinant of the Jacobian is given by

$$\det\left|\frac{d\mathbf{z}}{d\mathbf{w}}\right| = \det\mathbf{P} = (1+\mathbf{d}_{N+1}'\mathbf{d}_{N+1})^{-1/2},$$

where we have used Schur's formula: $\det(\mathbf{I} + \mathbf{d}_{N+1} \times \mathbf{d}_{N+1}') = 1 + \mathbf{d}_{N+1}'$. Completing the square in equation (A9), we can simplify $\mathbf{J}_{N+1}^1$ to

$$\mathbf{J}_{N+1}^1 = \frac{\phi\left(c/\sqrt{1+\mathbf{d}_{N+1}'\mathbf{d}_{N+1}}\right)}{\sqrt{1+\mathbf{d}_{N+1}'\mathbf{d}_{N+1}}}$$

$$\times \left(\int_{\mathbb{R}^N} \phi(\mathbf{w};\mathbf{0},\mathbf{I})\,(\mathbf{a}+\mathbf{P}\mathbf{w})'\mathbf{F}(\mathbf{a}+\mathbf{P}\mathbf{w})d\mathbf{w} - \epsilon\right).$$

Let $\mathbf{W}$ be a random variable with density $\phi(\mathbf{w};\mathbf{0},\mathbf{I})$ and $\mathbf{W}_i$ its components. Then,

$$\mathbb{E}[\mathbf{W}_i] = 0, \quad \mathbb{E}[\mathbf{W}_i\mathbf{W}_j] = \delta_{i,j}, \quad \mathbb{E}[\mathbf{W}_i\mathbf{W}_j\mathbf{W}_k] = 0,$$
$$\mathbb{E}[\mathbf{W}_i\mathbf{W}_j\mathbf{W}_k\mathbf{W}_l] = \delta_{i,j}\delta_{k,l} + \delta_{i,k}\delta_{j,l} + \delta_{i,l}\delta_{j,k},$$
$$\mathbb{E}[\mathbf{W}_i\mathbf{W}_j\mathbf{W}_k\mathbf{W}_l\mathbf{W}_m] = 0.$$

Thus, with λ given in the text, we have by brute-force algebra that

$$\mathbb{E}(\mathbf{a}+\mathbf{P}\mathbf{W})'\mathbf{F}(\mathbf{a}+\mathbf{P}\mathbf{W}) - tr(\mathbf{F}) = \lambda = \lambda(c_{N+1},\mathbf{d}_{N+1}),$$

and

$$\mathbf{J}_{N+1}^1 = \frac{\lambda(c_{N+1},\mathbf{d}_{N+1})}{\sqrt{1+\mathbf{d}_{N+1}'\mathbf{d}_{N+1}}}\,\phi\left(\frac{c_{N+1}}{\sqrt{1+\mathbf{d}_{N+1}'\mathbf{d}_{N+1}}}\right)$$

$$= \mathbf{J}^1(c_{N+1},\mathbf{d}_{N+1}).$$

For $\mathbf{J}_{N+1}^2$, similar changes of variable give

$$\mathbf{J}_{N+1}^2 = \frac{\phi\left(c_{N+1}/\sqrt{1+\mathbf{d}_{N+1}'\mathbf{d}_{N+1}}\right)}{\sqrt{1+\mathbf{d}_{N+1}'\mathbf{d}_{N+1}}}\left\{\epsilon^2\mathbb{E}\left[c+\epsilon+\mathbf{d}_{N+1}'(\mathbf{a}+\mathbf{PW})\right]\right.$$

$$-2\epsilon\mathbb{E}\left[(c+\epsilon+\mathbf{d}_{N+1}'(\mathbf{a}+\mathbf{PW}))((\mathbf{a}+\mathbf{PW})'\mathbf{F}(\mathbf{a}+\mathbf{PW}))\right]$$

$$\left.+\mathbb{E}\left[(c+\epsilon+\mathbf{d}_{N+1}'(\mathbf{a}+\mathbf{PW}))((\mathbf{a}+\mathbf{PW})'\mathbf{F}(\mathbf{a}+\mathbf{PW}))^2\right]\right\}.$$

After tedious calculations of the above expectation, we get that $\mathbf{J}_{N+1}^2 = \mathbf{J}^2(c_{N+1}, \mathbf{d}_{N+1})$ as in Proposition 3.3.

For $\mathbf{I}_0$, notice that

$$\mathbf{I}_0 = \int_{\mathbb{R}^N}\phi(\mathbf{y}; \mathbf{0}, \mathbf{\Sigma}_{11})\Phi\left(A(\mathbf{y}+v_0\mathbf{\Sigma}_{10})+v_0\sqrt{\Sigma_{x|y}}\right)d\mathbf{y}$$

$$\approx \int_{\mathbb{R}^N}\phi(\mathbf{y}; \mathbf{0}, \mathbf{\Sigma}_{11})\Phi\left((c+\epsilon+v_0\sqrt{\Sigma_{x|y}})+\mathbf{d}'(\mathbf{y}+v_0\mathbf{\Sigma}_{10})\right.$$

$$\left.+(\mathbf{y}+v_0\mathbf{\Sigma}_{10})'\mathbf{E}(\mathbf{y}+v_0\mathbf{\Sigma}_{10})\right)d\mathbf{y}$$

$$= \int_{\mathbb{R}^N}\phi(\mathbf{y}; \mathbf{0}, \mathbf{\Sigma}_{11})\Phi\left(c_0+\mathbf{d}_0'\mathbf{y}+\mathbf{y}'\mathbf{Ey}\right)d\mathbf{y}.$$

Comparing the last equation with equation (A4), we immediately get without any calculations that

$$\mathbf{I}_0 \approx \mathbf{J}^0(c_0, \mathbf{d}_0) + \mathbf{J}^1(c_0, \mathbf{d}_0) - \frac{1}{2}\mathbf{J}^2(c_0, \mathbf{d}_0).$$

Similarly, we get

$$\mathbf{I}_k = \int_{\mathbb{R}^N}\phi(\mathbf{y}; \mathbf{0}, \mathbf{\Sigma}_{11})\Phi\left(A(\mathbf{y}+v_k\mathbf{\Sigma}_{11}\mathbf{e}_k)\right)d\mathbf{y}$$

$$\approx \int_{\mathbb{R}^N}\phi(\mathbf{y}; \mathbf{0}, \mathbf{\Sigma}_{11})\Phi\left(c+\epsilon+\mathbf{d}'(\mathbf{y}+v_k\mathbf{\Sigma}_{11}\mathbf{e}_k)\right.$$

$$\left.+(\mathbf{y}+v_k\mathbf{\Sigma}_{11}\mathbf{e}_k)'\mathbf{E}(\mathbf{y}+v_k\mathbf{\Sigma}_{11}\mathbf{e}_k)\right)d\mathbf{y}$$

$$= \int_{\mathbb{R}^N}\phi(\mathbf{y}; \mathbf{0}, \mathbf{\Sigma}_{11})\Phi\left(c_k+\mathbf{d}_k'\mathbf{y}+\mathbf{y}'\mathbf{Ey}\right)d\mathbf{y}$$

$$\approx \mathbf{J}^0(c_k, \mathbf{d}_k) + \mathbf{J}^1(c_k, \mathbf{d}_k) - \frac{1}{2}\mathbf{J}^2(c_k, \mathbf{d}_k).$$

Proof of Proposition 3.4: By the definition of $\mathbf{P}$,

$$\mathbf{P}^2 = (\mathbf{I}+\mathbf{vv}')^{-1} = \mathbf{I}-\psi\mathbf{vv}',$$

where the last equality follows from the so-called updating formula (see, for example, Greene 2000). Or one could verify straightforwardly that $(\mathbf{I}+\mathbf{vv}')(\mathbf{I}-\psi\mathbf{vv}')=\mathbf{I}$. To see that $\mathbf{I}-\theta\mathbf{vv}'$ is the unique square root of $\mathbf{P}^2$, notice that $\mathbf{I}-\theta\mathbf{vv}'$ is symmetric, and $2\theta-\theta^2\mathbf{v}'\mathbf{v}=\psi$, so

$$(\mathbf{I}-\theta\mathbf{vv}')^2 = \mathbf{I}-(2\theta-\theta^2\mathbf{v}'\mathbf{v})\mathbf{vv}' = \mathbf{I}-\psi\mathbf{vv}'.$$

The other equations now follow from brute-force computations.

Proof of Proposition 3.5: Notice that

$$\Pi = e^{-rT}\int_{\mathbb{R}^N}\phi(\mathbf{y}; \mathbf{0}, \mathbf{\Sigma}_{11})d\mathbf{y}$$

$$\times \int_{\underline{x}(\mathbf{y})}^{\infty}\left(e^{v_0 x+\mu_0}-\sum_{k=1}^{N}e^{v_k y_k+\mu_k}-K\right)\phi(x; \mu_{x|y}, \Sigma_{x|y})dx.$$

Thus,

$$\frac{\partial\Pi}{\partial s_0} = e^{-rT}\frac{\partial\mu_0}{\partial s_0}\int_{\mathbb{R}^N}\phi(\mathbf{y}; \mathbf{0}, \mathbf{\Sigma}_{11})d\mathbf{y}$$

$$\times \int_{\underline{x}(\mathbf{y})}^{\infty}e^{v_0 x+\mu_0}\phi(x; \mu_{x|y}, \Sigma_{x|y})dx$$

$$- e^{-rT}\int_{\mathbb{R}^N}\phi(\mathbf{y}; \mathbf{0}, \mathbf{\Sigma}_{11})\left(e^{v_0\underline{x}(\mathbf{y})+\mu_0}-\sum_{k=1}^{N}e^{v_k y_k+\mu_k}-K\right)$$

$$\times \frac{\partial\underline{x}(\mathbf{y})}{\partial s_0}\phi(\underline{x}(\mathbf{y}); \mu_{x|y}, \Sigma_{x|y})d\mathbf{y} = \frac{\partial\mu_0}{\partial s_0}\mathbf{S}_0\mathbf{I}_0.$$

The other deltas and kappa can be proven similarly. The two special cases can be obtained by using equations (45) and (46).

Appendix B: Implementation of the second-order boundary approximation

While it is very straightforward to implement the second-order boundary approximation, an efficient implementation which minimizes the computing time requires some effort. Below we comment on some of the details of the actual implementation along with some useful tricks:

1. $\mathbf{\Sigma}_{11}^{-1}\mathbf{\Sigma}_{10}$.
   Matrix inversion is a costly operation and should be avoided. Instead, we use matrix division to find the solution $\mathbf{z}$ of $\mathbf{\Sigma}_{10}=\mathbf{\Sigma}_{11}\mathbf{z}$. Because $\mathbf{\Sigma}_{11}$ is positive definite and symmetric, Cholesky factorization is useful in solving the linear system. Alternatively, one could use Gaussian elimination. The quantity $\mathbf{\Sigma}_{11}^{-1}\mathbf{\Sigma}_{10}$ is referred to in the computation of $\Sigma_{x|y}$, $\mathbf{d}$ and many other places.

2. $\mathbf{\Sigma}_{11}^{1/2}$.
   Notice that since $\mathbf{\Sigma}_{11}$ is positively definite and symmetric, an efficient algorithm to compute its square root is through the similarity transformation $\mathbf{\Sigma}_{11}=\mathbf{Q}'\mathbf{\Lambda}\mathbf{Q}$, where $\mathbf{Q}$ contains all the eigenvectors of $\mathbf{\Sigma}_{11}$ and $\mathbf{\Lambda}$ is a diagonal matrix containing all the corresponding eigenvalues. Then the square root of $\mathbf{\Sigma}_{11}$ is given by $\mathbf{\Sigma}_{11}^{1/2}=\mathbf{Q}'\mathbf{\Lambda}^{1/2}\mathbf{Q}$. Efficient algorithm for performing similarity transformation of a positive definite and symmetric matrix exists.

3. $tr(\mathbf{F}^2)$.
   Once the matrix $\mathbf{F}$ is computed from equation (36), we can avoid computing $\mathbf{F}^2$ by computing $tr(\mathbf{F}^2)$ as follows:

$$tr(\mathbf{F}^2) = \sum_{i=1}^{N}\sum_{j=1}^{N}\left[\mathbf{F}_{ij}\right]^2.$$

The right-hand side can be computed very efficiently by first taking the element-by-element square of $\mathbf{F}$ and then taking the sum of all the elements. This is computationally more efficient than computing the matrix $\mathbf{F}^2$ because

the former involves N^2 multiplications of two real numbers while the latter involves N^3 multiplications.

4. $\mathbf{v'v}$, $\mathbf{v'Fv}$ and $\mathbf{v'F^2v}$.

Define a $(N+2) \times N$ matrix $\mathbf{D}$ as follows

$$\mathbf{D} = (\mathbf{d}_0, \mathbf{d}_1, \ldots, \mathbf{d}_N, \mathbf{d}_{N+1})'.$$

Notice that we need to compute $\mathbf{v'v}$, $\mathbf{v'Fv}$ and $\mathbf{v'F^2v}$ for $\mathbf{v} = \mathbf{d}_i$ for $i = 0, 1, \ldots, N+1$. It is extremely useful to treat the scalars $\mathbf{v'v}$, $\mathbf{v'Fv}$ and $\mathbf{v'F^2v}$ as vectors, where the index is for $\mathbf{v}$ ranging from $\mathbf{d}_0$ to $\mathbf{d}_{N+1}$. All the equations below should be interpreted this way.

We use the following identities to compute the vectors $\mathbf{v'v}$, $\mathbf{v'Fv}$ and $\mathbf{v'F^2v}$:

$$\mathbf{v'v} = \text{rowsum}(\mathbf{D}^{\cdot 2}), \tag{A11}$$

$$\mathbf{v'Fv} = \text{diag}(\mathbf{DFD'}), \tag{A12}$$

$$\mathbf{v'F^2v} = \text{rowsum}((\mathbf{DF})^{\cdot 2}), \tag{A13}$$

where rowsum is the operator of taking the row sum of a matrix and $\mathbf{A}^{\cdot 2}$ stands for the element-by-element square of a matrix $\mathbf{A}$. Written out component-wise, we have

$$(\mathbf{d}_i)'\mathbf{d}_i = \sum_{j=1}^{N} (\mathbf{D}_{ij})^2, \tag{A14}$$

$$(\mathbf{d}_i)'\mathbf{Fd}_i = (\mathbf{DFD'})_{ii}, \tag{A15}$$

$$(\mathbf{d}_i)'\mathbf{F^2d}_i = \sum_{j=1}^{N} [(\mathbf{DF})_{ij}]^2. \tag{A16}$$

Equations (A14), (A15) and (A16) can be seen easily by noticing that $\mathbf{F}$ is symmetric.

5. **Vectorization**.

It is very important to use a vectorization technique in the actual implementation to avoid for-loops in the program and further improve the efficiency. This is especially important when N is large. All the scalar quantities involving $\mathbf{v}$, such as $\psi(\mathbf{v})$, $\theta(\mathbf{v})$, $\mathbf{v'v}$, $\mathbf{v'Fv}$, $\mathbf{v'F^2v}$, $tr[(\mathbf{PFP})^2]$, $\mathbf{v'P^2FP^2v}$, and $\|\mathbf{PFP^2v}\|^2$ should be treated as $(N+2) \times 1$ vectors, where the index is on $\mathbf{v}$ ranging from $\mathbf{d}_0$ to $\mathbf{d}_{N+1}$. In particular, this means that we should use equations (A11), (A12) and (A13) instead of (A14), (A15) and (A16). Furthermore, $\lambda(u, \mathbf{v})$, $\mathbf{J}^0(u, \mathbf{v})$, $\mathbf{J}^1(u, \mathbf{v})$ and $\mathbf{J}^2(u, \mathbf{v})$ should be treated as $(N+2) \times 1$ vectors where u ranges from c_0 to c_{N+1} and $\mathbf{v}$ ranges from $\mathbf{d}_0$ to $\mathbf{d}_{N+1}$. Equation (24) then allows us to treat $\mathbf{I}$ as a $(N+2) \times 1$ vector. In turn, the spread option price in equation (23) is simply given by

$$\Pi = \mathbf{S}_0\mathbf{I}_0 - \sum_{k=1}^{N} \mathbf{S}_k\mathbf{I}_k - Ke^{-rT}\,\mathbf{I}_{N+1} = \mathbf{S'I}.$$

Despite its seemingly complexity, the second-order boundary approximation is very straightforward to implement and our code in MATLAB is only about 30 lines. The second-order boundary approximation is also extremely fast and the computation of $\Sigma_{11}^{1/2}$ is actually where more than half of the computing time is spent. For example, when $N = 50$, the second-order boundary approximation needs less than 3×10^{-3} s to compute the price of one spread option and the computation of $\Sigma_{11}^{1/2}$ takes about 1.8×10^{-3} s.